Available online at www.sciencedirect.com

ScienceDirect

European Journal of Protistology 77 (2021) 125763

European Journal of PROTISTOLOGY

www.elsevier.com/locate/ejop

Morphology and ontogenesis of two new *Hemiholosticha* species (Ciliophora, Hypotrichia, Hemiholostichidae nov. fam.)

Peter Vďačný[a,*], Wilhelm Foissner[b]

[a] *Department of Zoology, Faculty of Natural Sciences, Comenius University in Bratislava, Ilkovičova 6, 842 15 Bratislava, Slovakia*
[b] *Department of Biosciences, Faculty of Natural Sciences, Paris Lodron University of Salzburg, Hellbrunnerstrasse 34, 5020 Salzburg, Austria*

Received 15 July 2020; received in revised form 3 November 2020; accepted 22 November 2020
Available online 30 November 2020

Abstract

The morphology and ontogenesis of two new hypotrich ciliates, *Hemiholosticha solitaria* and *Hemiholosticha germanica*, were studied using live observation, protargol impregnation, and scanning electron microscopy. Both species share a medium-sized, almost globular body with a short anterior projection; two macronuclear nodules with a single micronucleus in between; a central contractile vacuole; three or four ventral, one postoral, one right and one left marginal cirral row; and three dorsal kineties extending along ribs. However, *H. germanica* is distinguished from congeners by a higher number of cirri in ventral rows R1 and R2 (3–6 vs. 2 cirri in each row). *Hemiholosticha solitaria* differs from congeners by having four (vs. three) ventral cirral rows and by the lack (vs. presence) of intracellular green algae. The ontogenesis of *H. solitaria* follows the *H. pantanalensis* mode in that (i) the oral primordium develops in a deep pouch and generates the first two cirral streaks in addition to adoral membranelles and undulating membranes, (ii) the undulating membrane anlage does not produce any cirri, and (iii) the longitudinal ventral cirral row R3 originates from two anlagen. The ontogenetic peculiarities along with the 18S rRNA gene phylogenies suggest classification of *Hemiholosticha*, *Psilotrichides*, and *Urospinula* into a new family, Hemiholostichidae.

© 2020 Elsevier GmbH. All rights reserved.

Keywords: *Hemiholosticha germanica* nov. spec.; *Hemiholosticha solitaria* nov. spec.; Hemiholostichidae nov. fam.; Intracellular green algae; Pantanal; Wetland

Introduction

The genus *Hemiholosticha* Gelei, 1954 was assigned to the hypotrich family Psilotrichidae Bütschli, 1889 by Heber et al. (2014). Psilotrichids are very interesting from the phylogenetic, ontogenetic, and ecological points of view (Heber et al. 2014; Luo et al. 2019; Vďačný and Foissner 2019). As concerns their phylogenetic position, psilotrichids, represented by *Hemiholosticha*, *Psilotrichides* Heber et al., 2018, and *Urospinula* Corliss, 1960, form a monophyletic lineage classified in a soft polytomy of the subclass Hypotrichia Stein, 1859 in the 18S rRNA gene analyses (Heber et al. 2014; Luo et al. 2019). Recently, Luu et al. (2020) showed that *Psilotricha* Stein, 1859, the type genus of the Psilotrichidae, does not group with *Hemiholosticha*, *Psilotrichides*, and *Urospinula*, and erroneously suggested exclusion of the nominotypical genus from the family Psilotrichidae. Ontogenesis of *Psilotricha* is not known and that of *Hemiholosticha*, *Psilotrichides*, and *Urospinula* exhibits a mixture of features found not only in various groups of hypotrichs (amphisiellids, kahliellids, oxytrichids, and schmidingerothrichids) but also in other spirotrich subclasses (euplotids and oligotrichs)

*Corresponding author.
E-mail address: peter.vdacny@uniba.sk (P. Vďačný).

https://doi.org/10.1016/j.ejop.2020.125763
0932-4739/© 2020 Elsevier GmbH. All rights reserved.

(Foissner 1983; Heber et al. 2014; Vďačný and Foissner 2019). Such a composite nature of ontogenesis indicates that the convergent evolution of morphogenetic processes might be a rather common phenomenon in hypotrichs (for reviews, see Berger 1999, 2006, 2008, 2011). And, finally, the type species of *Psilotricha* and further three genera assigned to the Psilotrichidae display associations with various colourless and/or green members of the order Chlamydomonadales from the class Chlorophyceae. The character of this relationship is still not known, and it has been speculated that the intracellular chlamydomonads might represent a selective prey of psilotrichids or an early stage of endosymbiosis (Heber et al. 2014; Kahl 1932; Kreutz 2008; Luo et al. 2019; Stein 1859; Vďačný and Foissner 2019).

The genus *Hemiholosticha* was re-defined and taxonomically revised by Heber et al. (2014). It belongs to the small ciliate genera, since it includes only three species hitherto: *H. kahli* Luo et al., 2019 [= *Psilotricha viridis* (Penard, 1922>) sensu Kahl (1932) according to Luo et al. (2019)]; *H. pantanalensis* Foissner and Vďačný in Vďačný and Foissner (2019); and *H. viridis* Gelei, 1954. All three species share a globular to broadly obovate body, two macronuclear nodules with a single micronucleus in between, a contractile vacuole situated near the body centre, conspicuously long frontal membranelles, and a distinctly curved (cyrtohymenid) paroral membrane. The ontogenesis of *Hemiholosticha* is characterised by a combination of the following features: the postoral cirral row is ontogenetically active; the oral primordium generates first two cirral streaks in addition to adoral membranelles and undulating membranes; the parental undulating membranes are reorganised; and the longitudinal ventral cirral row R3 originates from two anlagen (Heber et al. 2014; Vďačný and Foissner 2019).

In the present study, we describe two further *Hemiholosticha* species, *H. solitaria* nov. spec. and *H. germanica* nov. spec. The former taxon contains colourless chlamydomonads and was discovered in a soil sample taken from the Pantanal wetland in Brazil. On the other hand, the latter species carries intracellular green algae with red eyespot in addition to colourless chlamydomonads and was discovered in an aquatic sample from the Simmelried mire in Germany. Since *H. solitaria* grew very well in raw cultures, we obtained enough dividers to study its ontogenesis as well. Our comparative analyses reveal that although *Hemiholosticha* species share a rather similar interphase cirral pattern, they could differ even in the number of the cirral streak anlagen and in the migration routes of some cirri. The new findings show that the genus *Hemiholosticha* might still harbour multiple undescribed species and that just the peak of an iceberg of the hypotrich diversity has been described so far (Foissner 2016; Foissner et al. 2002; Hu et al. 2009; Liu et al. 2017).

Another aim of this study is to solve the classification problem of *Hemiholosticha* and its relatives, as they do not cluster with the type genus of the family Psilotrichidae (Luu et al. 2020). The genetic data along with a combination of ontogenetical peculiarities suggest that *Hemiholosticha*, *Psilotrichides*, and *Urospinula* need to be classified in a new family.

Material and methods

Sampling and sample processing

Hemiholosticha solitaria nov. spec. was discovered in the same sample as *H. pantanalensis*, i.e., in dusty, light brown soil mixed with some litter and fine roots. The sample was collected in the surroundings of kilometre 42 of the Transpantaneira Road between the cities of Poconé and Porto Jofre, near the Pousada Rio Claro, Pantanal wetland, Mato Grosso, Brazil, S16°39′ W56°45′ by Maria Pichler and Birgit Weissenbacher (Vďačný and Foissner 2019). It was air-dried for three weeks and sealed in a plastic bag. Ciliates were reactivated from resting cysts, using the non-flooded Petri dish method (Vďačný and Foissner 2012). To obtain enough morphostatic specimens and dividers, raw cultures were set up in Eau de Volvic (French table water) with a few millilitres of the eluate from the non-flooded Petri dish culture and some crashed wheat kernels to stimulate the growth of bacteria and protists.

Hemiholosticha germanica nov. spec. originated from an aquatic sample collected in the Simmelried. This is an approximately three hectare-sized wetland near the village of Hegne, which belongs to the town of Constance, Germany, N47°43′03.0″ E9°05′36.6″ (Kreutz and Foissner 2006). The sample was collected by Martin Kreutz and pooled into a 10-litre aquarium containing water and organic debris from the Simmelried mire. *Hemiholosticha germanica* reached high abundances in the water column of the aquarium, from where it was collected by a plankton net. Unfortunately, no specimens were stored for molecular analyses because both species were discovered almost 15 yr ago when molecular characterization of ciliates just began.

Taxonomic methods and terminology

Morphology of both *Hemiholosticha* species was studied using a combination of in vivo observation, protargol impregnation, and scanning electron microscopy (SEM), as described by Foissner (1991, 2014). Living cells were examined using a high-power oil immersion objective and differential interference contrast microscopy. Protargol impregnation followed protocol A. Da Fano solution was used for fixation of *H. solitaria*, while ethanol for fixation of *H. germanica*. The ontogenetic processes of *H. solitaria* were reconstructed from protargol preparations, which show concomitantly body shape, ciliary pattern, and nuclear apparatus.

In vivo measurements were performed with an ocular micrometre at a magnification of 25–1000×, while counts

and measurements on protargol-impregnated specimens were conducted at a magnification of 1250×. Illustrations of live specimens were based on free-hand sketches and photographs, while those of impregnated cells were made with a drawing device. To illustrate the changes during the morphogenetic processes, parental cirri were depicted by contour, whereas new ones were shaded black.

General terminology follows Lynn (2008). Morphostatic terminology is based on Berger (1999, 2006, 2008, 2011) and Heber et al. (2014). Ontogenetic terminology is according to Foissner (1996) and the numbering of cirral streaks is according to Heber et al. (2014) and Vďačný and Foissner (2019). Division stages are distinguished as follows: early dividers are characterised by the macronucleus composed of two nodules occupying the central quarters of the cell. In mid-dividers, the macronuclear nodules are fused into a central mass. Late dividers are constricted in the middle and have a dumbbell-shaped macronucleus.

ZooBank registration number of the work (Recommendation 8A of the International Commission on Zoological Nomenclature, 2012) is urn:lsid:zoobank.org:pub:7FC8E09B-3029−4A50-A168−49BFF2613961.

Phylogenetic methods

To infer the phylogenetic positions of *Hemiholosticha*, *Psilotricha*, *Psilotrichides*, and *Urospinula* within the subclass Hypotrichia, 18S rRNA gene sequences of 102 hypotrich and three oligotrich ciliates (serving as outgroup) were retrieved from GenBank (https://www.ncbi.nlm.nih.gov/genbank/). Their accession numbers are shown in the respective figure. Taxon sampling mostly followed Jung and Berger (2019) and Luo et al. (2019). The 18S rRNA gene sequences were aligned on the MAFFT ver. 7 server (https://mafft.cbrc.jp/alignment/server/) (Katoh et al. 2019), using the Q-ins-I strategy, the 200PAM/κ = 2 scoring matrix, the gap opening penalty at 1.53, and no effect of Ns on the alignment score.

The maximum likelihood tree was constructed with the program IQTree (Nguyen et al. 2015) on XSEDE ver. 1.6.10 as implemented on the CIPRES portal ver. 3.3 (http://www.phylo.org/) (Miller et al. 2010). The best fitting evolutionary substitution model was determined with the aid of the BIC criterion, using the in-built ModelFinder program. The maximum likelihood analyses included the BioNJ tree option to build the starting tree, correction for ascertainment bias, 1000 ultrafast bootstrap replicates to assess the reliability of internal nodes, and the bnni algorithm to reduce overestimating support (Hoang et al. 2018).

Prior to conducting Bayesian analyses, the best evolutionary substitution model was selected under the BIC criterion in jModelTest ver. 2.1.10 (Darriba et al. 2012) on the CIPRES portal. Bayesian inference was carried out in the program MrBayes on XSEDE ver. 3.2.7 (Ronquist et al. 2012) also on the CIPRES server. More specifically, MCMC simulations included two independent runs each with four simultaneous chains, five million generations, a sampling frequency of trees and parameters at one hundred, a burn-in fraction of first 25% of sampled trees, and the GTR + I + Γ evolutionary model with the following prior parameter values: base frequencies A = 0.2679, C = 0.1888, G = 0.2541, T = 0.2892; rate matrix for the substitution model [AC] = 1.2267, [AG] = 3.2744, [AT] = 1.4156, [CG] = 0.7248, [CT] = 5.8694, [GT] = 1.0000; proportion of invariable sites I = 0.6050; and the gamma distribution shape parameter Γ = 0.4610. Convergence of the Markov Chain Monte Carlo (MCMC) analyses to the stationary distribution and an adequate sample from the posterior distribution were confirmed using the in-built diagnostics (i.e., the average standard deviation of split frequencies was <0.01, the potential scale reduction factor was 1, the effective sample sizes were >200, and no obvious trends were in the plots of generations versus log probability).

Weighted Kishino-Hasegawa test was carried out in order to assess differences in log likelihoods between the best tree in which *Psilotricha* does not group with *Hemiholosticha*, *Psilotrichides*, and *Urospinula*, and the alternative tree in which all four genera cluster together. The best unconstraint as well as the constraint tree were built in the program IQTree with the same settings as described above. Topology testing was performed with 10 000 re-samplings using the RELL method. The number, type, and localization of primary nucleotide homologies supporting the best and alternative groupings of psilotrichids were determined with the help of the on-line tool DeSignate (https://designate.dbresearch.uni-salzburg.at/) (Hütter et al. 2020).

Results

Hemiholosticha solitaria nov. spec.

ZooBank registration number

urn:lsid:zoobank.org:act:C31B1E4F-7AD8−4D7B-94A6-D335E66A3 F41.

Diagnosis

Size in vivo about 80 × 70 μm; body almost globular to broadly obovate with short anterior projection at distal end of adoral zone; dorsal side with three distinct ribs. Two ellipsoid macronuclear nodules and a single micronucleus in between. On average a total of 47 cirri in four ventral, one postoral, one right and one left marginal row. On average 31 dorsal bristles in three kineties, posterior bristles elongated. Adoral zone extends about 50% of body length, composed of an average of 21 membranelles.

Table 1. Morphometric data on *Hemiholosticha solitaria* (S) nov. spec. and *Hemiholosticha germanica* (G) nov. spec.

Characteristic[a]	Taxon	Mean	M	SD	SE	CV	Min	Max	n
Body, length	S	58.4	59.0	5.5	0.9	9.5	48.0	69.0	37
	G	48.2	48.0	3.4	0.7	7.1	43.0	56.0	25
Body, width	S	47.5	48.0	4.6	0.8	9.6	37.0	57.0	37
	G	33.6	34.0	3.6	0.7	10.7	28.0	43.0	25
Body length:width, ratio	S	1.2	1.2	0.1	0.0	7.2	1.1	1.4	37
	G	1.4	1.5	0.1	0.0	8.4	1.2	1.6	25
Anterior projection, height	S	3.1	3.0	0.9	0.2	28.7	2.0	4.0	21
	G	1.8	2.0	0.6	0.1	35.5	1.0	3.0	21
Macronuclear nodules, number	S	2.0	2.0	0.0	0.0	0.0	2.0	2.0	21
	G[b]	2.0	2.0	0.0	0.0	0.0	2.0	2.0	23
Micronuclei, number	S[c]	1.0	1.0	0.0	0.0	0.0	1.0	1.0	21
	G[d]	1.0	1.0	0.0	0.0	0.0	1.0	1.0	21
Anterior body end to anterior nodule, distance	S	12.8	13.0	1.5	0.3	11.5	10.0	16.0	21
	G	9.9	10.0	1.6	0.3	16.1	6.0	13.0	21
Macronuclear nodules, distance in between	S	4.3	5.0	1.5	0.3	34.7	2.0	7.0	21
	G	3.1	3.0	1.3	0.3	40.7	1.0	5.0	21
Anterior macronuclear nodule, length	S	12.9	13.0	2.2	0.5	16.8	7.0	16.0	21
	G	10.5	10.0	1.2	0.3	11.1	9.0	12.0	21
Anterior macronuclear nodule, width	S	8.9	9.0	1.5	0.3	17.2	5.0	11.0	21
	G	8.1	8.0	0.9	0.2	11.7	6.0	10.0	21
Anterior macronuclear nodule length:width, ratio	S	1.5	1.4	0.2	0.1	15.9	1.1	2.0	21
	G	1.3	1.3	0.2	0.1	17.4	1.0	1.8	21
Nucleoli, maximum diameter	S	3.0	3.0	0.0	0.0	0.0	3.0	3.0	4
	G	2.9	3.0	0.7	0.2	23.8	2.0	4.0	18
Micronucleus, length	S	4.5	4.5	0.5	0.1	10.5	4.0	5.0	21
	G	3.1	3.0	0.4	0.1	13.3	2.5	4.0	21
Micronucleus, width	S	3.0	3.0	0.4	0.1	13.6	2.0	4.0	21
	G	2.7	2.5	0.3	0.1	10.8	2.0	3.0	21
Micronucleus length:width ratio	S	1.5	1.4	0.3	0.1	17.7	1.0	2.0	21
	G	1.2	1.2	0.2	0.0	18.7	1.0	2.0	21
Anterior body end to proximal end of AZM, length	S	29.7	30.0	1.7	0.4	5.7	27.0	33.0	21
	G	24.9	25.0	1.5	0.3	6.2	21.0	28.0	21
Adoral zone of membranelles, % of body length	S	50.4	50.0	3.9	0.9	7.8	44.1	58.0	21
	G	51.6	51.0	3.2	0.7	6.2	47.7	59.1	21
Adoral membranelles, number	S	20.6	21.0	0.7	0.2	3.6	19.0	22.0	21
	G	18.5	18.0	0.8	0.2	4.4	17.0	20.0	21
Adoral membranelles, length of widest base	S	7.1	7.0	–	–	–	7.0	8.0	21
	G	6.2	6.0	–	–	–	6.0	7.0	21
Frontal adoral membranelles, length of cilia	S	19.7	20.0	2.4	0.9	12.3	16.0	22.0	7
	G	19.0	19.5	1.3	0.5	6.7	17.0	20.0	6
Buccal cavity, width	S	9.7	10.0	0.6	0.1	6.0	9.0	11.0	21
	G	6.9	7.0	1.4	0.3	20.9	4.0	9.0	21
Anterior body end to paroral membrane, distance	S	9.9	10.0	1.9	0.4	19.7	6.0	13.0	21
	G	4.8	5.0	1.2	0.3	25.1	3.0	7.0	21
Paroral membrane, length	S	16.1	16.0	1.3	0.3	8.1	14.0	19.0	21
	G	15.0	15.0	2.0	0.4	13.6	10.0	18.0	21
Anterior body end to endoral membrane, distance	S	13.2	13.0	2.4	0.5	18.5	10.0	19.0	21
	G	11.6	12.0	2.5	0.5	21.6	8.0	17.0	21

Table 1 (*Continued*)

Characteristic[a]	Taxon	Mean	M	SD	SE	CV	Min	Max	n
Endoral membrane, length	S	13.3	13.0	1.4	0.3	10.7	9.0	15.0	21
	G	10.5	10.0	2.0	0.4	19.5	6.0	15.0	21
Left marginal cirral row, number of cirri	S	7.7	7.0	1.0	0.2	13.3	6.0	9.0	21
	G	6.2	6.0	0.8	0.2	13.3	5.0	8.0	21
Postoral cirral row, number of cirri	S	6.7	7.0	1.1	0.2	16.4	3.0	8.0	21
	G	4.4	5.0	0.9	0.2	19.6	2.0	6.0	21
Anterior body end to postoral cirral row, distance	S	20.9	21.0	2.4	0.5	11.6	17.0	26.0	21
	G	20.0	19.0	3.1	0.7	15.7	16.0	26.0	21
Postoral cirral row, length	S	19.4	20.0	3.9	0.8	19.9	8.0	25.0	21
	G	15.0	15.0	3.9	0.8	25.8	5.0	21.0	21
Ventral cirral row R0, number of cirri	S	2.0	2.0	0.0	0.0	0.0	2.0	2.0	21
Ventral cirral row R1, number of cirri	S[e]	2.0	2.0	0.0	0.0	0.0	2.0	2.0	21
	G	5.0	5.0	0.4	0.1	8.9	4.0	6.0	21
Ventral cirral row R1, length	G	12.1	12.0	1.7	0.4	14.3	9.0	7.0	21
Anterior body end to posteriormost cirrus of ventral cirral row R1, distance	G	15.7	15.0	2.1	0.5	13.7	13.0	20.0	21
Ventral cirral row R2, number of cirri	S[f]	2.0	2.0	0.0	0.0	0.0	2.0	2.0	20
	G	3.9	4.0	0.5	0.1	12.4	3.0	5.0	21
Anterior body end to ventral cirral row R2, distance	S	11.8	11.0	2.2	0.5	18.6	9.0	17.0	21
Ventral cirral row R2, length	S	5.5	5.0	0.9	0.2	16.3	4.0	7.0	20
	G	12.8	13.0	2.2	0.5	17.5	8.0	18.0	21
Anterior body end to posteriormost cirrus of ventral cirral row R2, distance	G	18.1	17.0	3.0	0.7	16.8	13.0	26.0	21
Ventral cirral row R3, number of cirri	S	13.5	13.0	1.0	0.2	7.3	11.0	15.0	21
	G	10.9	11.0	1.0	0.2	9.6	10.0	13.0	21
Anterior body end to posterior portion of ventral cirral row R3, distance	G	13.5	13.0	2.2	0.5	16.1	9.0	17.0	21
Anterior portion of ventral cirral row R3, number of cirri	G	2.0	2.0	0.0	0.0	0.0	2.0	2.0	21
Posterior portion of ventral cirral row R3, number of cirri	G	8.9	9.0	1.0	0.2	11.7	8.0	11.0	21
Right marginal cirral row, number of cirri	S	12.7	13.0	1.4	0.3	11.0	10.0	15.0	21
	G	12.6	13.0	1.2	0.3	9.5	9.0	15.0	21
Cirri, total number	S[g]	46.2	47.0	3.1	0.7	6.8	38.0	50.0	19
	G	43.0	43.0	2.8	0.6	6.5	37.0	47.0	21
Cirri, length	S	17.7	18.0	2.2	0.7	12.4	13.0	20.0	11
	G	18.3	18.0	1.9	0.6	10.6	15.0	21.0	10
Dorsal kinety 1, number of bristles	S	9.9	10.0	1.2	0.3	12.3	8.0	13.0	21
	G	7.5	7.0	0.7	0.1	8.9	6.0	9.0	23
Anterior body end to dorsal kinety 1, distance	S	16.0	16.0	2.4	0.5	14.8	13.0	22.0	21
	G	15.7	15.0	2.9	0.6	18.7	12.0	24.0	23
Posterior body end to dorsal kinety 1, distance	G	8.0	8.0	1.9	0.4	24.1	4.0	11.0	23
Dorsal kinety 2, number of bristles	S	10.4	10.0	1.1	0.2	10.8	8.0	13.0	21
	G	10.9	11.0	1.0	0.2	9.5	9.0	13.0	23
Anterior body end to dorsal kinety 2, distance	S	11.9	11.0	2.3	0.5	19.3	9.0	19.0	21
	G	10.0	10.0	2.1	0.4	20.9	7.0	16.0	23
Dorsal kinety 3, number of bristles	S	11.8	11.0	1.1	0.2	9.3	10.0	14.0	21
	G	13.6	14.0	1.5	0.3	10.8	10.0	16.0	23

Table 1 (*Continued*)

Characteristic[a]	Taxon	Mean	M	SD	SE	CV	Min	Max	n
Anterior body end to dorsal kinety 3, distance	S	6.6	6.0	1.8	0.4	27.0	4.0	11.0	21
	G	4.6	4.0	1.2	0.3	26.8	3.0	7.0	23
Dorsal bristles, total number	S	32.1	31.0	3.0	0.7	9.4	27.0	39.0	21
	G	32.0	32.0	2.4	0.5	7.4	28.0	36.0	23
Posterior dorsal bristles, length	S	9.1	9.0	0.7	0.3	7.5	8.0	10.0	7
	G	6.4	7.0	1.2	0.4	18.6	5.0	8.0	8
Anterior dorsal bristles, length	S	4.0	4.0	0.0	0.0	0.0	4.0	4.0	9
	G	3.2	3.0	–	–	–	3.0	4.0	6

[a]Data based on mounted, protargol-impregnated, and randomly selected specimens from raw cultures. Measurements in μm. AZM – adoral zone of membranelles; CV – coefficient of variation (%); M – median; Max – maximum; Mean – arithmetic mean; Min – minimum; n – number of individuals investigated; SD – standard deviation; SE – standard error of arithmetic mean.

[b]Of 24 specimens investigated, one cell had a single macronuclear nodule and one cell had three nodules.

[c]Not recognizable in one out of 22 specimens.

[d]Not recognizable in three out of 24 specimens.

[e]Three cirri in one out of 21 specimens.

[f]One cirrus in one out of 21 specimens.

[g]Not including one, respectively, two supernumerary cirri in two out of 21 specimens.

Type locality

Dusty, light brown soil from the Pantanal wetland, Mato Grosso, Brazil, S16°39′ W56°45′.

Type material

The holotype slide (reg. no. 2020/15) and two paratype slides (reg. nos 2020/16, 17) with protargol-impregnated specimens have been deposited in the Museum of Natural History (Biologiezentrum) in Linz (LI), Austria. The holotype (Fig. 1G, H) and relevant paratype specimens as well as dividers have been marked by black ink circles on the coverslip.

Etymology

The species-group name *solitari·us -a, -um* [m, f, n] (lonely, lonesome) is a Latin adjective in nominative singular (Article 11.9.1.1 of the International Commission on Zoological Nomenclature, 1999) and refers to having no companion green intracellular algae, a typical feature of all other *Hemiholosticha* species.

Description

Size in vivo 50–110 × 40–80 μm, on average 80 × 70 μm, i.e., distinctly longer and wider than in protargol preparations (48–69 × 37–57 μm, on average 59 × 48 μm) very likely due to the fixation procedure (Table 1). Body almost globular to broadly obovate with a length:width ratio ranging from 1.1:1 to 1.4:1 in protargol preparations; a short anterior projection at distal end of adoral zone; posterior end broadly rounded but usually slightly narrower than anterior end; right cell margin very thin and hence appearing hyaline in vivo (Figs. 1A–C, G, 2A–C, 3A, 4A; Table 1). Dorsoventrally flattened up to 2:1, ventral side flat to slightly concave, dorsal side moderately convex and with three prominent ribs well recognizable in optical cross sections during live observation and usually not preserved in SEM photographs very likely due to preparation procedures (Figs. 1D, F, 2 C, 3A, 4A). Nuclear apparatus in central quarters of cell, almost in body midline; invariably composed of two macronuclear nodules and one micronucleus in between. Macronuclear nodules broadly ellipsoid, ellipsoid or ovoid with a length:width ratio of 1.1–2.0:1; size about 7–16 × 5–11 μm, usually about 13 × 9 μm in protargol preparations; distance between nodules highly variable (CV = 34.7%), ranging from 2 μm to 7 μm; nodules usually connected by a fine strand impregnated with protargol; nucleoli globular and up to 3 μm across. Micronucleus broadly ellipsoid to ellipsoid, i.e., about 4–5 × 2–4 μm, on average 4.5 × 3.0 μm in protargol preparations (Figs. 1H, 2D; Table 1). Contractile vacuole near body centre, with two collecting canals extending anteriorly and posteriorly (Fig. 1A, C). Cortex inflexible, colourless, lacks specific granules. Cytoplasm colourless; finely granulated; studded with lipid droplets and food vacuoles containing *Polytomella*-like flagellates (Figs. 1A, E, 2B, D). Swims moderately fast, creeps on soil particles, also rests on organic debris.

Cirri firm, thorn-like, up to 20 μm long in vivo, 13–20 μm (on average 18 μm) after protargol impregnation, and 9.5–15.0 μm in SEM; total number rather stable (CV = 6.8%) ranging from 38 to 50; arranged in four ventral, one postoral, one right and one left marginal row; frontal, buccal, and transverse cirri not distinguishable (Figs. 1G, 2C, 3A, 4A; Table 1). Ventral cirral rows R0 and R1 invariably composed of two cirri each, anterior cirrus of each row near distal end of adoral zone, posterior cirrus slightly anterior to mid-portion of paroral membrane. Ventral cirral row R2 begins 9–17 μm posterior to anterior body end; 4–7 μm long after protargol impregnation; typically composed of two cirri, rarely of one cirrus (in one out of 21 specimens). Ventral cirral row R3 conspicuously longer than R0–R2; extends from anterior

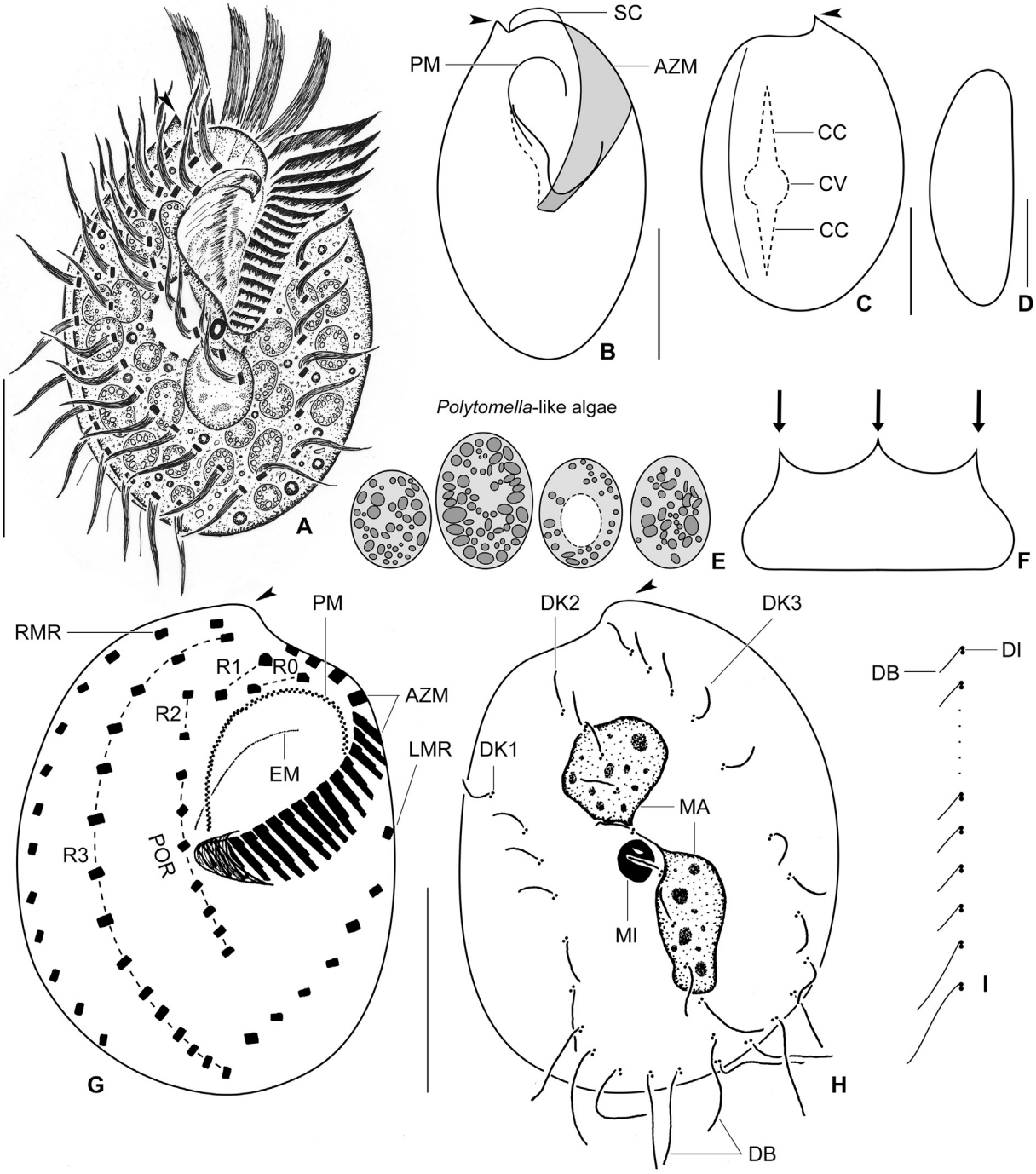

Fig. 1. (**A–I**) *Hemiholosticha solitaria* nov. spec. from life (A–F) and after protargol impregnation (G–I). Arrowhead in (A–C, G, H) marks the anterior body projection. (**A**) Ventral view of a representative specimen. (**B**) Shape variant. (**C, D**) Dorsal and lateral overviews. (**E**) Intracellular *Polytomella*-like algae. (**F**) Optical cross section, showing the three prominent dorsal ribs (arrows). (**G, H**) Ventral and dorsal view of ciliary pattern and nuclear apparatus of holotype specimen. (**I**) Semi-schematic diagram of a dorsal kinety. AZM, adoral zone of membranelles; CC, collecting canals; CV, contractile vacuole; DB, dorsal bristles; DK1–3, dorsal kineties; DI, dorsal dikinetids; EM, endoral membrane; LMR, left marginal cirral row; MA, macronuclear nodules; MI, micronucleus; PM, paroral membrane; POR, postoral cirral row; R0–3, ventral cirral rows; RMR, right marginal cirral row; SC, scutum. Scale bars: 20 μm (G, H) and 30 μm (A–D).

to posterior body end in slightly curved pattern; consists of 11–15 cirri, anterior cirri more widely spaced than posterior ones. Postoral cirral row begins slightly posterior to row R2 and extends to second third of body; 8–25 μm long after protargol impregnation; composed of three to eight, usually seven cirri. Right marginal cirral row begins near anterior body end, extends along body margin following its curvature to terminate near rear body end; consists of 10–15 cirri.

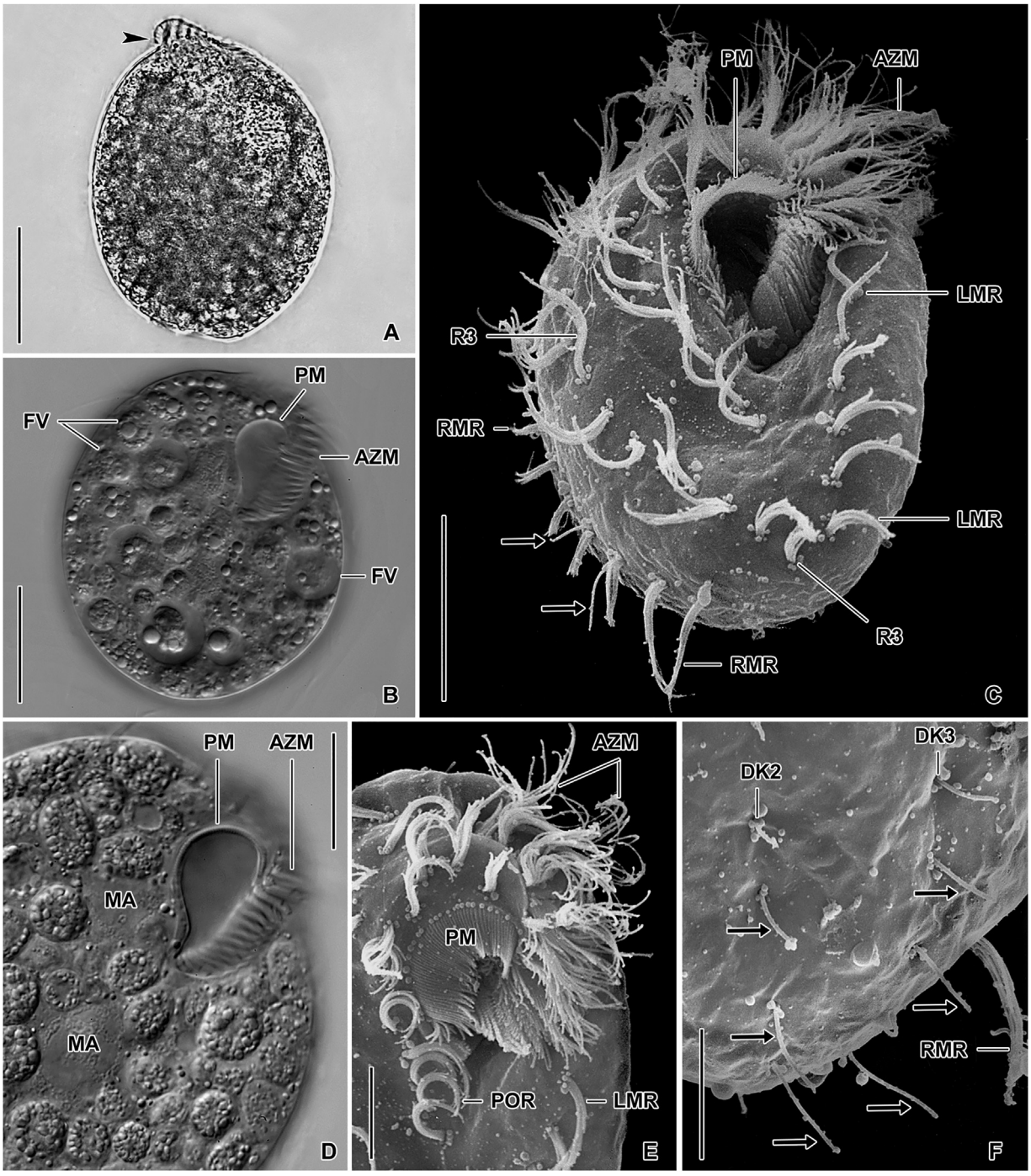

Fig. 2. (**A–F**) *Hemiholosticha solitaria* nov. spec. from life (A, B, D) and in the SEM (C, E, F). Arrowhead in (A) marks the scutum, arrows in (C, F) mark dorsal bristles. (**A**) Dorsal overview, showing the scutum (arrowhead). (**B, C**) Ventral overviews, showing the general body organization and the cirral pattern. (**D, E**) Ventral view of the anterior body half, showing the *Cyrtohymena*-like paroral membrane. (**F**) Dorsal view of the posterior body region. Note that dorsal bristles (arrows) gradually increase in length and the posteriormost bristles protrude beyond the rear body end. AZM, adoral zone of membranelles; DK2, 3, dorsal kineties; FV, food vacuoles; LMR, left marginal cirral row; MA, macronuclear nodules; PM, paroral membrane; POR, postoral cirral row; R3, ventral cirral row 3; RMR, right marginal cirral row. Scale bars: 10 μm (E, F), 20 μm (C, D), and 30 μm (A, B).

Left marginal cirral row commences at level of mid-portion of adoral zone and terminates at level of rear end of right marginal cirral row; composed of six to nine cirri (Figs. 1G, 2C, 3A, 4A; Table 1).

Dorsal bristles fine, increase in length from 4 μm anteriorly to 8–10 μm posteriorly; total number of bristles ranging from 27 to 39 (CV = 9.4%); arranged in three meridional rows; posteriormost bristles protrude beyond rear body end. Dorsal

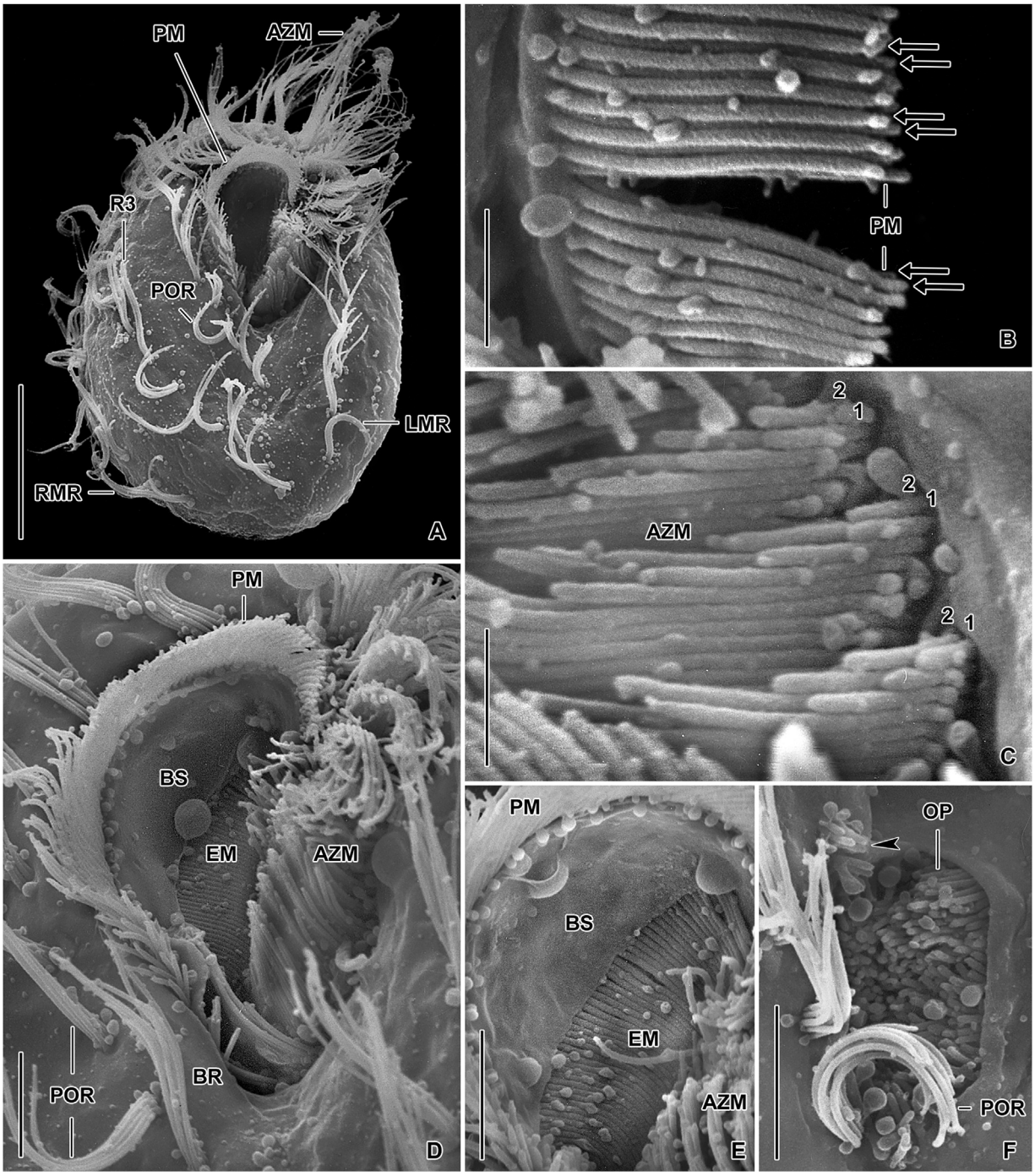

Fig. 3. (**A–F**) *Hemiholosticha solitaria* nov. spec. in the SEM. (**A**) Ventral overview. (**B**) Detail of the paroral membrane. Note that both basal bodies of oral dikinetids are ciliated (arrows). (**C**) Detail of the left side of adoral membranelles. (**D, E**) Details of the oral apparatus, showing the crook-like paroral, the buccal seal, and the endoral whose cilia form a plate-like structure at the bottom of the buccal cavity. (**F**) The oral primordium develops near the posterior postoral cirri in a pouch. Arrowhead marks some short cilia that do not sink into the pouch but remain on its right margin very likely to form the opisthe's undulating membranes. 1, 2, long rows of adoral membranelle; AZM, adoral zone of membranelles; BR, buccal ridge; BS, buccal seal; LMR, left marginal cirral row; OP, oral primordium; PM, paroral membrane; POR, postoral cirral row; R3, ventral cirral row 3; RMR, right marginal cirral row. Scale bars: 2 μm (B, C), 5 μm (D–F), and 20 μm (A).

kineties extend in furrows left of ribs. Dorsal kinety 1 begins in first third of body length, composed of 8–13 bristles. Dorsal kinety 2 commences subapically, consists of 8–13 bristles. Dorsal kinety 3 starts slightly below to anterior body end, consists of 10–14 bristles. Caudal cirri absent (Figs. 1H, I, 2F, 4C; Table 1).

Adoral zone extends about 50% of body length on average; commences anteriorly near midline of body and forms

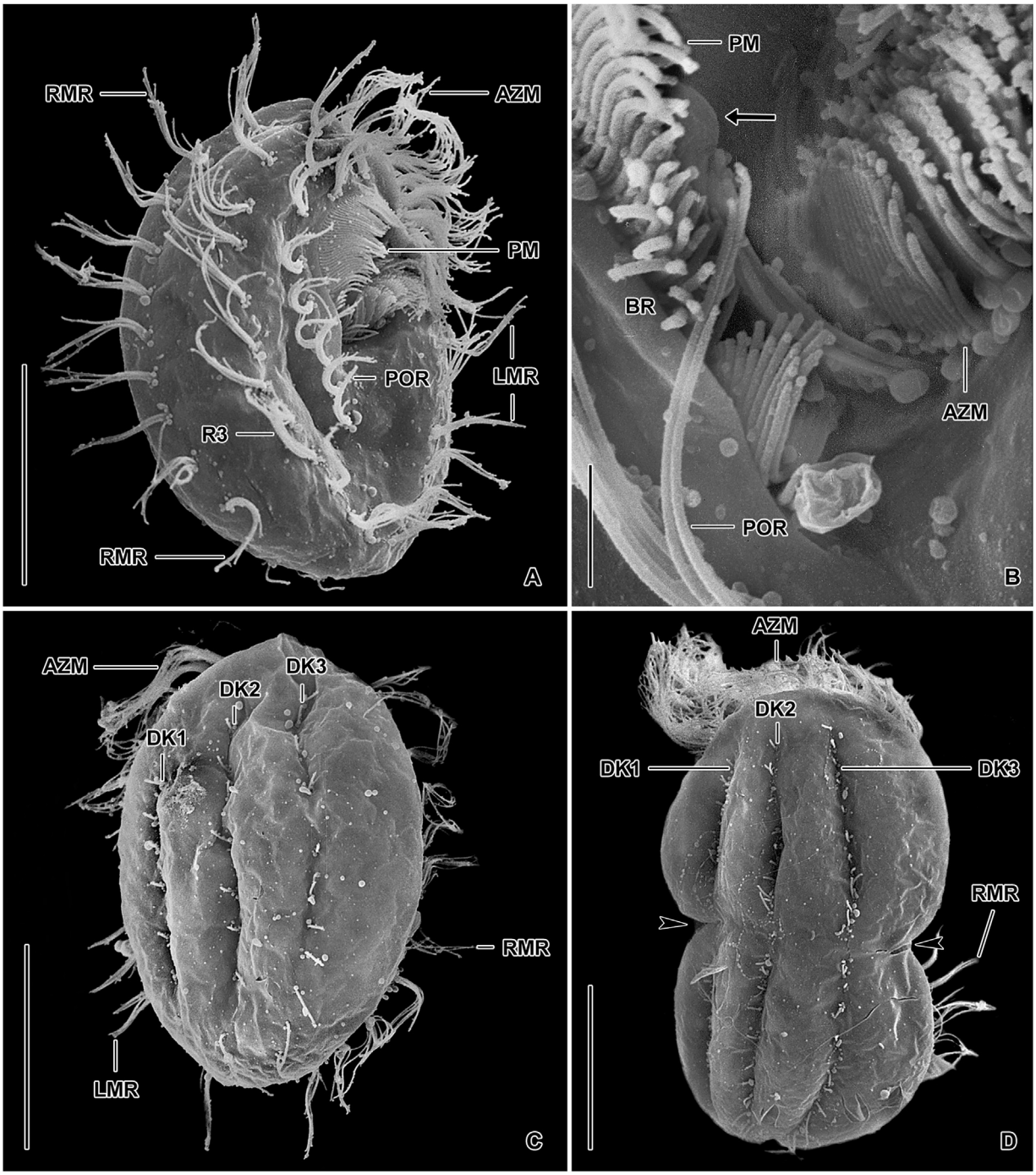

Fig. 4. (**A–D**) *Hemiholosticha solitaria* nov. spec. in the SEM. (**A**) Ventral overview, showing the general body organization and the cirral pattern. (**B**) Detail of the proximal end of the oral apparatus. Note that both basal bodies of the paroral dikinetids are ciliated and the posterior end of the paroral is very likely triplicated. Adoral membranelles are composed of four rows of basal bodies, but only cilia of the two long rows are recognizable. Arrow marks the buccal seal. (**C, D**) Dorsal overview of a morphostatic specimen and a late divider. Opposed arrowheads mark the prospective fission area. AZM, adoral zone of membranelles; BR, buccal ridge; DK1–3, dorsal kineties; LMR, left marginal cirral row; PM, paroral membrane; POR, postoral cirral row; R3, ventral cirral row 3; RMR, right marginal cirral row. Scale bars: 3 μm (B) and 30 μm (A, C, D).

a question mark-like pattern in ventral view; composed of an average of 21 membranelles. Individual membranelles composed of four rows of basal bodies: rows 1 and 2 long, bear cilia whose length increases from 5 μm to 16–22 μm in distal half of adoral zone, causing conspicuous frontal membranelles; row 3 slightly shorter than rows 1 and 2; row 4 very short, bears minute cilia recognizable only in some well-oriented specimens; largest bases of membranelles 7–8 μm

wide after protargol impregnation (Figs. 1A, B, G, 2B–E, 3A, C, D, 4A, B; Table 1). Scutum crescentic, minute, i.e., about 3 μm high in vivo, emerges slightly anterior to beginning of ventral cirral row R1 and merges into margin of membranellar stripe partially covering frontal membranelles (Figs. 1B, 2A, C, E, 4A).

Buccal cavity almost as long as ventral portion of adoral zone; about 9–11 μm wide in protargol preparations; right margin elevates into a conspicuous C-shaped ridge anteriorly merging into scutum and posteriorly into buccal vertex (Figs. 2B–D, 3A, D, E; Table 1). Paroral membrane begins about 10 μm posterior to anterior body end; extends crook-like over buccal ridge, resembling the cyrtohymenid pattern; about 16 μm long in protargol preparations and shorter than adoral zone proximally and distally; composed of narrowly spaced dikinetids, both basal bodies ciliated according to SEM observations (Fig. 3B, arrows); cilia 10–15 μm long in vivo, gradually decreasing to 7 μm at both ends; posterior portion rarely triplicated according to SEM observations (Figs. 1B, G, 2B–E, 3A, B, D, 4A, B; Table 1). Endoral membrane begins above mid of buccal cavity, i.e., about 13 μm posterior to anterior body end; optically intersects paroral membrane and terminates at level of its proximal end; about 13 μm long in protargol preparations; composed of densely spaced basal bodies; cilia 4.0–4.5 μm long in SEM, form a plate-like structure at bottom of buccal cavity indicating that they might be motionless (Figs. 1G, 3D, E; Table 1). Buccal seal recognizable in some well-preserved specimens (Fig. 3D, E).

Ontogenesis of *Hemiholosticha solitaria*

Division mode

Binary fission is homothetogenic and occurs in freely motile condition as usual for psilotrichids and the majority of hypotrichs. Stomatogenesis is apokinetal and the parental oral structures are not involved in the formation of the daughter oral ciliature, although the parental undulating membranes are reorganised.

Adoral zone of membranelles and undulating membranes

Stomatogenesis commences with apokinetal (de novo) proliferation of basal bodies close to the rearmost postoral cirri, i.e., near to the buccal vertex (Fig. 5A, C). The growing anarchic field invaginates into a deep pouch, which contains densely and irregularly arranged basal bodies of the prospective adoral membranelles (Fig. 5B, D). The growing cilia of the protomembranelles are covered by the cortex and only some are visible through the ovate opening of the pouch in the SEM micrographs (Fig. 3F). However, the parental postoral cirri and some densely arranged basal bodies bearing short cilia do not sink into the pouch but remain on its right margin (Fig. 3F, arrowhead). According to protargol preparations, these narrowly spaced basal bodies are very likely derived from the right anterior portion of the oral primordium (Fig. 5D, arrow) and will form a long, curved dikinetidal streak, i.e., the anlage for the undulating membranes of the opisthe. In the meantime, new adoral membranelles differentiate from the growing oral primordium in a posteriad direction, forming a zone that extends between the posterior portion of the parental adoral zone and the left marginal cirral row (Fig. 5G, F). The opisthe's adoral zone is fully developed already in mid-dividers (Fig. 6A). Formation of the new paroral and the new endoral membrane is also accomplished in mid-dividers by splitting the opisthe's undulating membrane anlage (Fig. 6A). However, both membranes attain their specific morphology and position in late dividers (Fig. 6E).

The parental adoral zone does not show any sign of reorganization. On the other hand, the parental undulating membranes begin with their reorganization already in early dividers, i.e., when the formation of the opisthe's adoral zone of membranelles is almost completed (Fig. 5F, G, asterisk). In mid-dividers, the new proter's undulating membranes are arranged in parallel and have a similar length (Fig. 6A). The species-specific *Cyrtohymena*-like pattern is obtained in late dividers (Fig. 6E).

Cirral streaks

Four streaks of basal bodies develop both in the proter and the opisthe. In the proter, streak I forms near and possibly from the posterior cirrus of parental ventral row R0; streak II develops near and possibly from the posterior cirrus of parental ventral row R1; and streaks III and IV form in a V-shaped pattern within parental ventral row R3 (Fig. 5F, G). In the opisthe, streaks I and II are derived from the opisthe's undulating membrane anlage (Fig. 5E, F); streaks III and IV develop in a V-shaped pattern within parental ventral row R3 posterior to proter's streaks III and IV (Fig. 5F, G). All streaks elongate posteriorly and start to produce cirri in a posteriad direction already in early dividers (Fig. 5F, G). Streak I generates two cirri of ventral row R0; streak II forms two cirri of ventral row R1; streak III first splits two anteriormost cirri that migrate leftwards and anteriorly to form the ventral row R2 (Fig. 6A, C, E, arrows), then it splits four or five further cirri that migrate rightwards and anteriorly to become the anterior part of ventral row R3 (Fig. 6A, C, E, arrowheads), and the remaining cirri migrate leftwards and posteriorly to become the postoral row; streak IV contributes the posterior portion of ventral row R3 (Fig. 6A, C, E). The new cirral rows obtain their species-specific positions in late dividers. The majority of parental cirri becomes resorbed in late dividers (Fig. 6E).

Marginal and dorsal anlagen

Formation of new marginal cirral rows and dorsal kineties proceeds as usual for psilotrichids. Briefly, the proter's left and right marginal row anlagen develop at the anterior end of the parental marginal cirral rows, very likely by dissociation of their anteriormost cirri. The opisthe's left and right marginal row anlagen are formed within the parental marginal cirral rows at about level of the oral primordium.

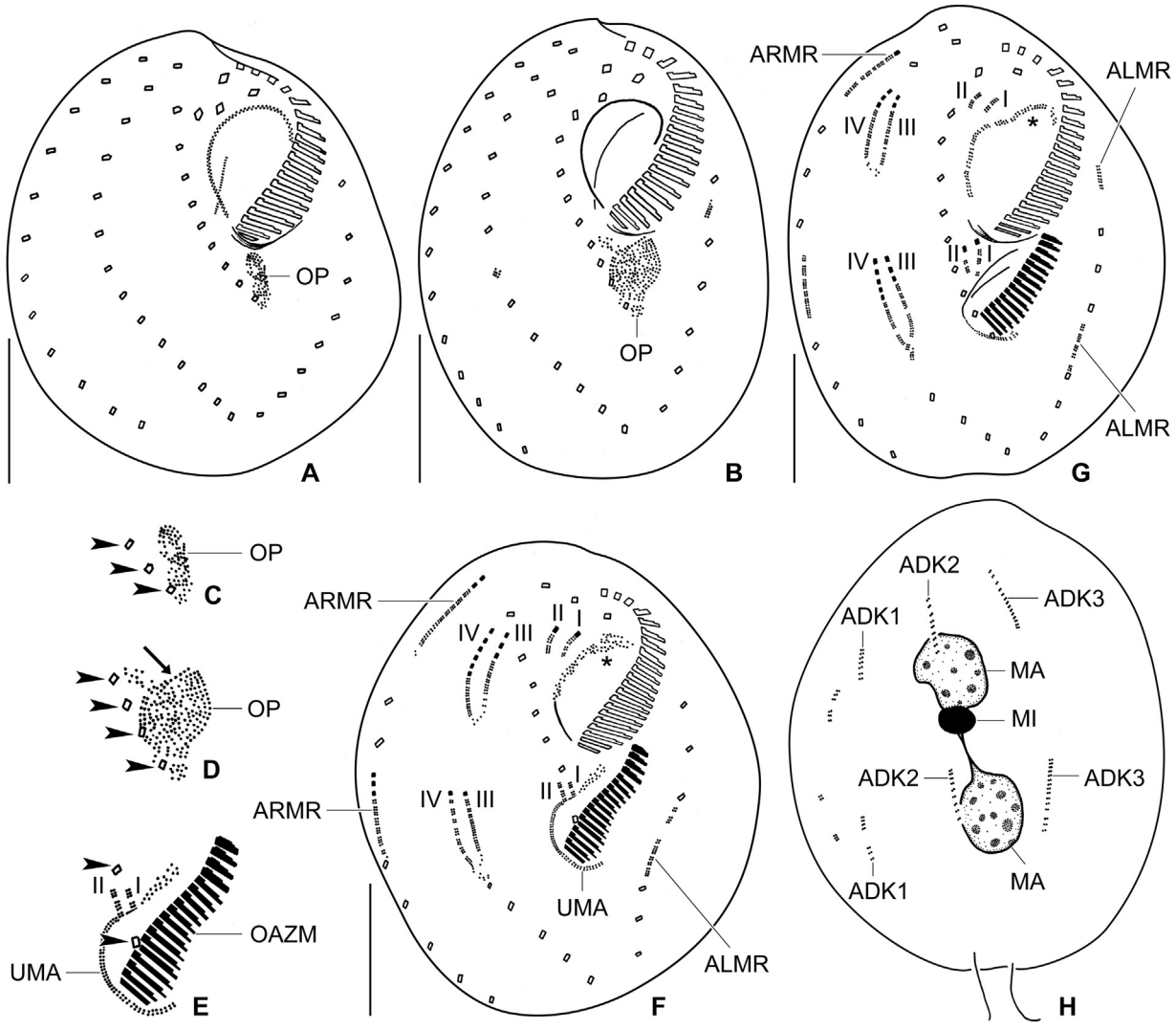

Fig. 5. (**A–H**) *Hemiholosticha solitaria* nov. spec., ciliary pattern and nuclear apparatus of early dividers after protargol impregnation. Parental cirri and adoral membranelles are depicted by contour, while new ones are shaded black. Arrow in (D) marks the undulating membrane anlage, arrowheads in (C–E) denote the posterior postoral cirri, and asterisk in (G, F) marks the reorganizing parental undulating membranes. (**A, B**) Ventral view of very early dividers, showing the oral primordium close to the posteriormost postoral cirri, i.e., just posterior of the buccal vertex. (**C, D**) Details of the oral primordium of specimens shown in (A, B). The oral primordium develops in a deep pouch, as typical of psilotrichids, and consists of densely and irregularly arranged basal bodies that will produce the opisthe's adoral zone of membranelles and the undulating membrane anlage. (**E**) Detail of the opisthe's oral apparatus of the specimen shown in (F). Note that cirral streaks I and II develop from the undulating membrane anlage. (**F, G**) Ventral view of early dividers, showing four cirral streaks both in proter and opisthe. In the proter, streak I forms near and possibly from the posterior cirrus of parental ventral row R0, streak II develops near and possibly from the posterior cirrus of parental ventral row R1, and streaks III and IV form in a V-shaped pattern within parental ventral row R3. In the opisthe, streaks I and II are derived from the opisthe's undulating membrane anlage, and streaks III and IV develop in a V-shaped pattern within parental ventral row R3 posterior to proter's streaks III and IV. Formation of new marginal cirral rows proceeds as usual for hypotrichs. Specifically, the proter's left and right marginal cirral row anlagen develop at the anterior end of the parental marginal cirral rows. The opisthe's left and right marginal cirral row anlagen are formed within the parental marginal cirral rows at the level of the growing oral primordium. The marginal cirral row anlagen gradually produce new cirri posteriorly. (**H**) Dorsal view of the same specimen shown in (G). Morphogenesis of the dorsal ciliature very likely begins by formation of within-row primordia in dorsal kineties at two sites, anterior and posterior to the fission area. The new dorsal kineties reach their final length and structure in mid-dividers. I–IV, cirral streaks; ADK1–3, anlagen of dorsal kineties; ALMR, anlagen of left marginal cirral row; ARMR, anlagen of right marginal cirral row; MA, macronuclear nodules; MI, micronucleus; OAZM, opisthe's adoral zone of membranelles; OP, oral primordium; UMA, undulating membrane anlage. Scale bars: 20 μm.

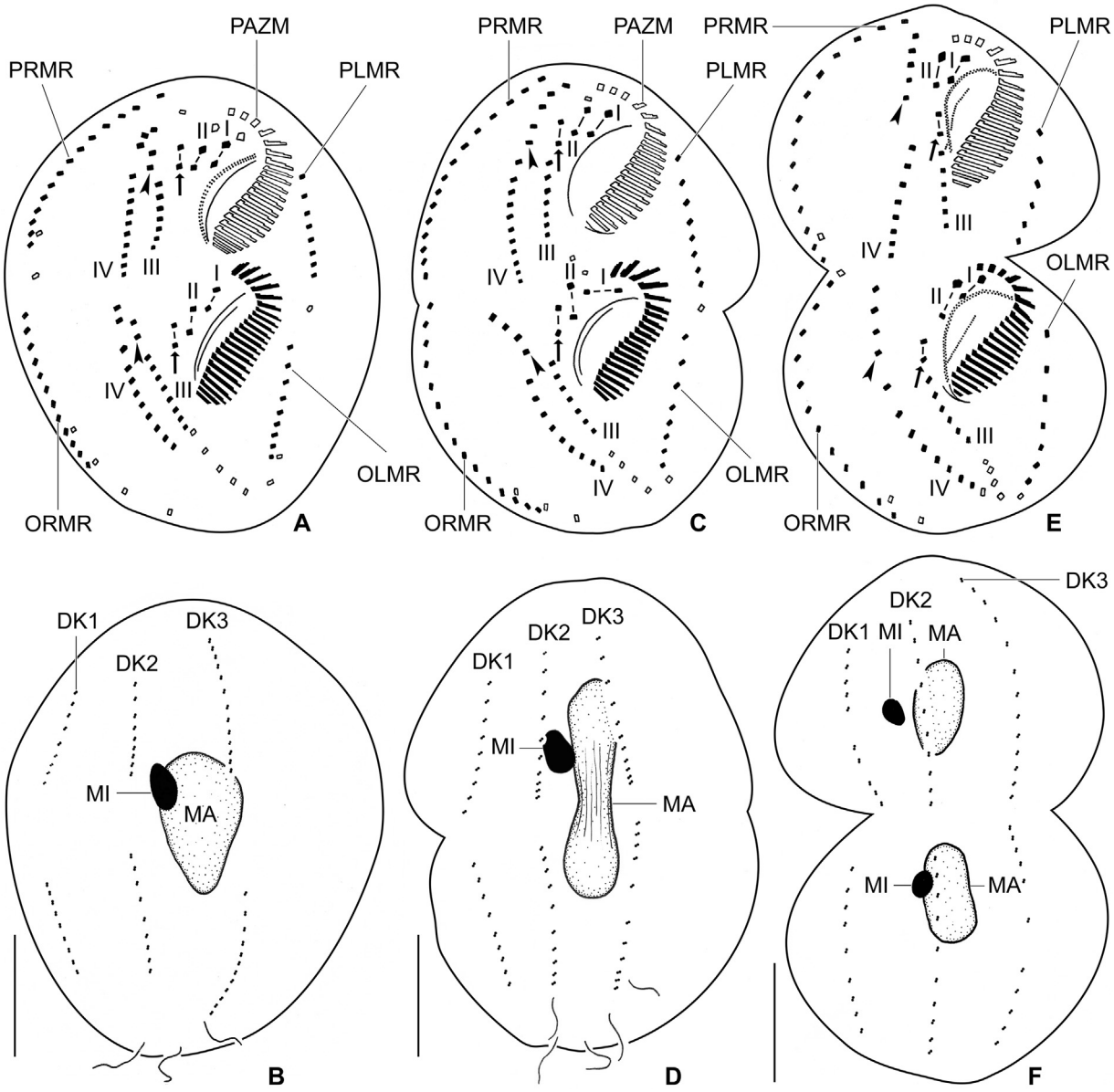

Fig. 6. (**A–F**) *Hemiholosticha solitaria* nov. spec., ciliary pattern and nuclear apparatus of mid-dividers (A–D) and a late divider (E, F) after protargol impregnation. Parental cirri and adoral membranelles are depicted by contour, while new ones are shaded black. Arrows in (A, C, E) mark the first two cirri of streak III that migrate leftwards and anteriorly to form the ventral row R2, arrowheads in (A, C, E) mark cirri of streak III that migrate rightwards and anteriorly to become the anterior part of ventral row R3. (**A, C, E**) Ventral view of mid-dividers and a late divider to show the cirri and migration pattern. Streak I generates two cirri of ventral row R0, streak II forms two cirri of ventral row R1, streak III first splits two anteriormost cirri that migrate leftwards and anteriorly to form the ventral row R2 (arrows), then splits four or five further cirri that migrate rightwards and anteriorly to become the anterior part of ventral row R3 (arrowheads) and its remaining cirri migrate leftwards and posteriorly to become the postoral row, streak IV contributes the remainder cirri of the posterior portion of ventral row R3. The new cirral rows obtain their species-specific positions in late dividers. In mid-dividers, the new undulating membranes are arranged in parallel and have a similar length. The species specific *Cyrtohymena*-like pattern is obtained in late dividers. (**B, D, F**) Dorsal view of mid-dividers and a late divider. The new dorsal kineties get their specific number of basal bodies already in mid-dividers but obtain their characteristic positions in late dividers. I–IV, cirral streaks; DK1–3, dorsal kineties; MA, macronucleus; MI, micronucleus; OAZM, opisthe's adoral zone of membranelles; OLMR, opisthe's left marginal cirral row; ORMR, opisthe's right marginal cirral row; PAZM, proter's adoral zone of membranelles; PLMR, proter's left marginal cirral row; PRMR, proter's right marginal cirral row. Scale bars: 20 μm.

The marginal row anlagen extend posteriorly, gradually producing new cirri already in early dividers (Fig. 5F, G). The parental marginal cirri are almost completely resorbed and replaced by new cirri during the mid- and late division stages (Fig. 6A, C, E).

Morphogenesis of the dorsal side ciliature begins already in early dividers. Resorption of parental dorsal kineties takes place very early, causing that the onset of dorsal morphogenesis was not observed. Primordia of new dorsal kineties form very likely within the parental dorsal kineties at two sites, as indicated by an unciliated region anterior and posterior to the prospective fission area (Fig. 5H). Some extra dikinetids of an unknown origin were observed left of dorsal kinety 1 in a single early divider (Fig. 5H), but were not seen in mid-dividers and late dividers. The new dorsal kineties get their specific number of basal bodies already in mid-dividers (Fig. 6B) and obtain their characteristic positions in late dividers (Figs. 4D, 6D, F).

Nuclear division

The nuclear apparatus divides as typical for bimacronucleate hypotrichs. Specifically, in mid-dividers, both nodules fuse into a centrally located mass (Fig. 6B), which elongates (Fig. 6D) and divides into two oblong and pointed pieces (Fig. 6F). Each piece then divides once in post-dividers, producing two macronuclear nodules.

The micronucleus divides only once during the middle and late stages of binary fission (cp. Fig. 6B, D, with 6F). The daughter micronuclei move to the species-specific position in post-dividers when the formation of two macronuclear nodules is accomplished.

Hemiholosticha germanica nov. spec.

2008 *Psilotricha viridis* – Kreutz, Mikrokosmos 97, 328 (detailed in vivo observations).

2019 *Hemiholosticha kahli* nov. spec. – Luo et al., BMC Evol. Biol. 19: 8/15, pro parte, namely *Psilotricha viridis* sensu Kreutz (2008); not type population from Guam and not *Psilotricha viridis* sensu Kahl (1932).

ZooBank registration number

urn:lsid:zoobank.org:act:927EA6D4−8401-49CD-B68A-219C53A4FDD5.

Diagnosis

Size in vivo about 85 × 65 μm; body almost globular to broadly obovate with short anterior projection at distal end of adoral zone; dorsal side with three distinct ribs. Two ellipsoid macronuclear nodules and a single micronucleus in between. On average a total of 43 cirri in three ventral, one postoral, one right and one left marginal row. On average 32 dorsal bristles in three kineties, posterior bristles elongated. Adoral zone extends about 51% of body length, composed of an average of 18 membranelles. Green intracellular algae with eyespot present.

Type locality

Simmelried mire near the village of Hegne, Constance, Germany, N47°43′03.0″ E9°05′36.6″.

Type material

The holotype slide (reg. no. 2020/18) and the paratype slide (reg. no. 2020/19) with protargol-impregnated specimens have been deposited in the Museum of Natural History (Biologiezentrum) in Linz (LI), Austria. The holotype (Fig. 7B, C) and relevant paratype specimens have been marked by black ink circles on the coverslip.

Etymology

The species-group name *germanic·us -a, -um* [m, f, n] (German) is a Latin adjective in nominative singular (Article 11.9.1.1 of the International Commission on Zoological Nomenclature, 1999) and refers to the country where the new species was discovered.

Description

Size in vivo 75–95 × 55–75 μm, on average 85 × 65 μm, i.e., distinctly longer and wider than in protargol preparations (43–56 × 28–43 μm, on average 48 × 34 μm) very likely due to the fixation procedure (Table 1). Body almost globular to broadly obovate with a length:width ratio ranging from 1.2:1 to 1.6:1 in protargol preparations; a short anterior projection at distal end of adoral zone; posterior end broadly rounded but usually slightly narrower than anterior end; right cell margin very thin and hence appearing hyaline in vivo; dorsal side with three prominent ribs (Figs. 7A–C, H–K, 8A, B, D, 9A–D, 10 A, B; Table 1). Nuclear apparatus in central quarters of cell, almost in body midline; usually composed of two macronuclear nodules and one micronucleus in between. Macronuclear nodules globular to ellipsoid or ovoid, with a length:width ratio of 1.0–1.8:1; size about 9–12 × 6–10 μm, usually about 10.5 × 8.0 μm in protargol preparations; distance between nodules highly variable (CV = 40.7%), ranging from 1 μm to 5 μm; nodules usually connected by a fine strand impregnated with protargol; nucleoli globular to dumbbell-shaped and up to 4 μm across. Micronucleus globular to ellipsoid, i.e., about 2.5–4.0 × 2.0–3.0 μm, on average 3.1 × 2.7 μm in protargol preparations (Figs. 7C, K, 8C, 9A, C, D; Table 1). Contractile vacuole near body centre (Fig. 7A). Cortex inflexible, colourless, lacks specific granules. Cytoplasm colourless but cells appear greenish due to numerous green algae; finely granulated and studded with lipid droplets (Fig. 8A–C). Algae almost fill ciliate's body, four shape and size types recognizable: type I about 7–13 μm long, ellipsoid to narrowly ellipsoid, often with anterior papilla, chloroplast large and almost completely encircling cell, with subapical intraplastidial red eyespot (stigma) and starch granules (Figs. 7D, 8 C); type II similar to type I but larger (14–20 μm long) and

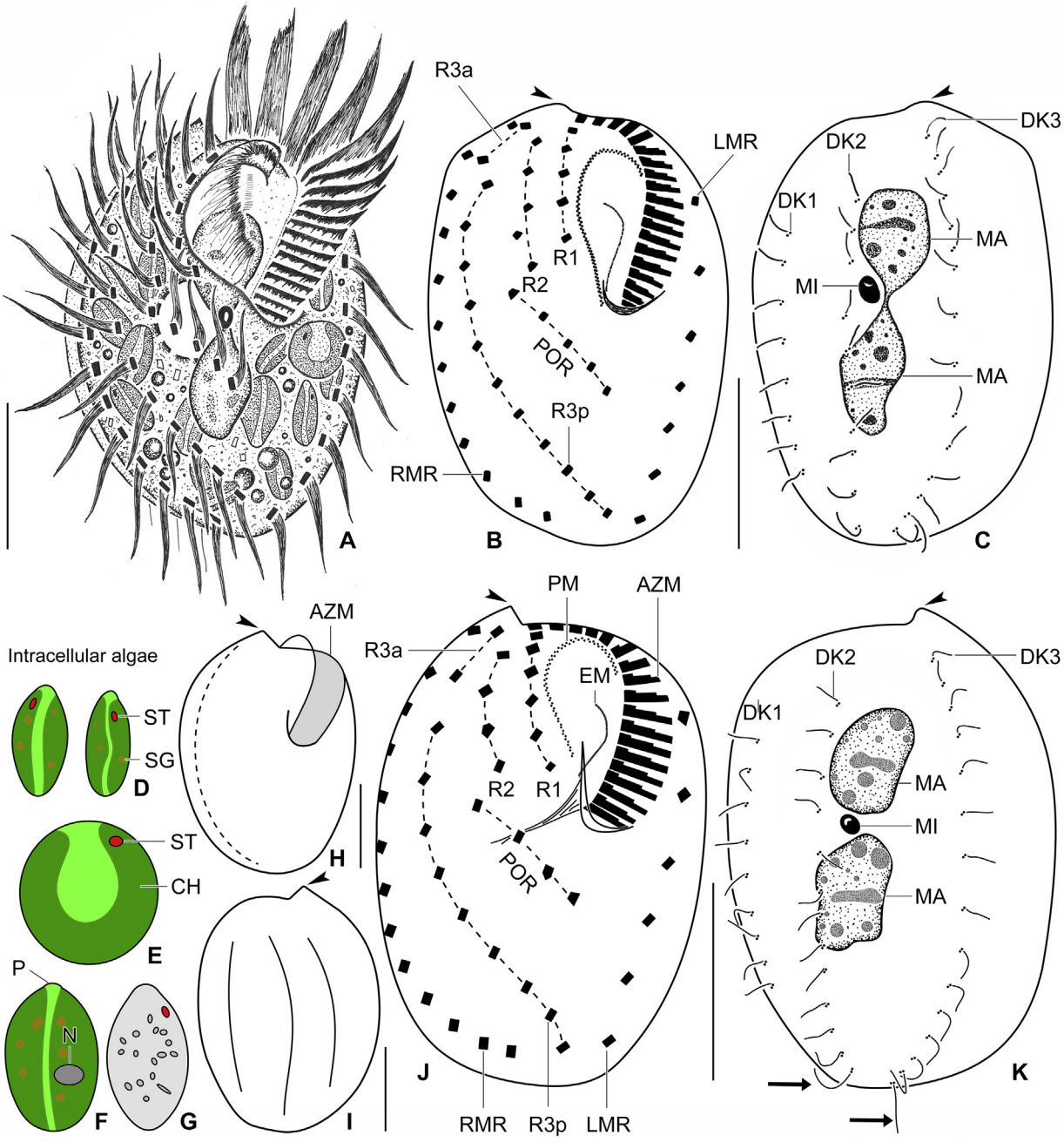

Fig. 7. (**A–K**) *Hemiholosticha germanica* nov. spec. from life (A, D–I) and after protargol impregnation (B, C, J, K). Arrowhead in (B, C, H–K) marks the anterior projection. (**A**) Ventral view of a representative specimen. (**B, C, J, K**) Ventral and dorsal view of ciliary pattern and nuclear apparatus in holotype (B, C) and in a paratype (J, K) specimen. Arrows in (K) mark the long dorsal bristles. (**D–G**) There are four types of intracellular algae. Type I is about 7–13 μm long, ellipsoid to narrowly ellipsoid, with large chloroplast containing a red eyespot (D). Type II is similar but larger (14–20 μm long) (F). Type III is about 5–23 μm in diameter and contains a cup-shaped chloroplast with red eyespot (E). Type IV is about 14–22 μm long, ellipsoid to narrowly ellipsoid. Its chloroplast is rudimentary or resorbed (G). (**H**) Shape variant. (**I**) Dorsal overview, showing three ribs. AZM, adoral zone of membranelles; CH, chloroplast; DK1–3, dorsal kineties; EM, endoral membrane; LMR, left marginal cirral row; MA, macronuclear nodules; MI, micronucleus; N, nucleus; P, anterior papilla; PM, paroral membrane; POR, postoral cirral row; R1, 2, ventral cirral rows 1 and 2; R3a, 3p, anterior and posterior portion of ventral cirral row 3; RMR, right marginal cirral row; SG, starch granules; ST, stigma. Scale bars: 20 μm (B, C, J, K) and 30 μm (A, H, I).

often without red eyespot (Fig. 7F); type III almost globular and about 5–23 μm in diameter, chloroplast large and cup-shaped, with subapical red eyespot (Fig. 7E); type IV about 14–22 μm long, ellipsoid to narrowly ellipsoid, often with anterior papilla, chloroplast rudimentary or resorbed, red eyespot rarely present, very likely corresponds to green forms in various stages of digestion (Fig. 7G). Glides and swims moderately fast.

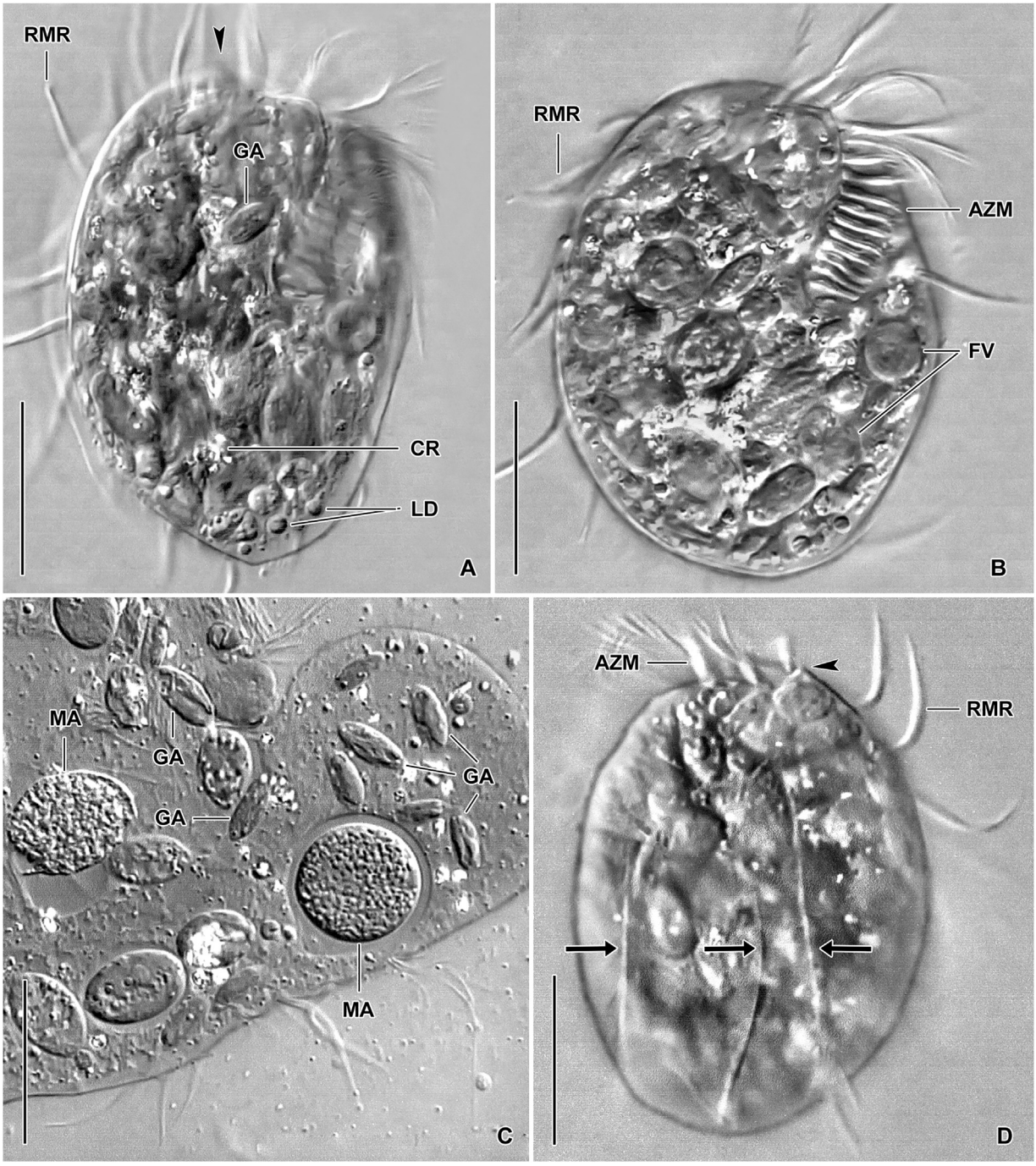

Fig. 8. (**A–D**) *Hemiholosticha germanica* nov. spec. from life. Arrowhead in (A, D) marks the anterior body projection. (**A, B**) Ventral overviews, showing the general body organization. The body is almost globular to broadly obovate, with a short anterior projection at the distal end of the adoral zone. The posterior body end is broadly rounded but usually slightly narrower than the anterior end. The adoral zone of membranelles occupies about half of the body length, commences anteriorly near the midline of the body, and forms a question mark-like pattern. (**C**) The cytoplasm is finely granulated, contains two macronuclear nodules, some lipid droplets, crystals and numerous green algae. (**D**) Dorsal overview, showing the three prominent longitudinal ribs (arrows). Photographs kindly supplied by Martin Kreutz. AZM, adoral zone of membranelles; CR, crystals; FV, food vacuoles; GA, green intracellular algae; LD, lipid droplets; MA, macronuclear nodules; RMR, right marginal cirral row. Scale bars: 20 μm (C) and 30 μm (A, B, D).

Cirri firm, thorn-like, 15–21 μm (on average 18 μm) after protargol impregnation; total number ranging from 37 to 47 (CV = 6.5%); arranged in three ventral, one postoral, one right and one left marginal row; frontal, buccal, and transverse cirri not distinguishable (Figs. 7B, J, 9 A, B, 10 A, B; Table 1). Ventral cirral row R1 composed of four to six cirri, begins near distal end of adoral zone and extends to level of mid-portion of paroral membrane. Ventral cirral row R2 con-

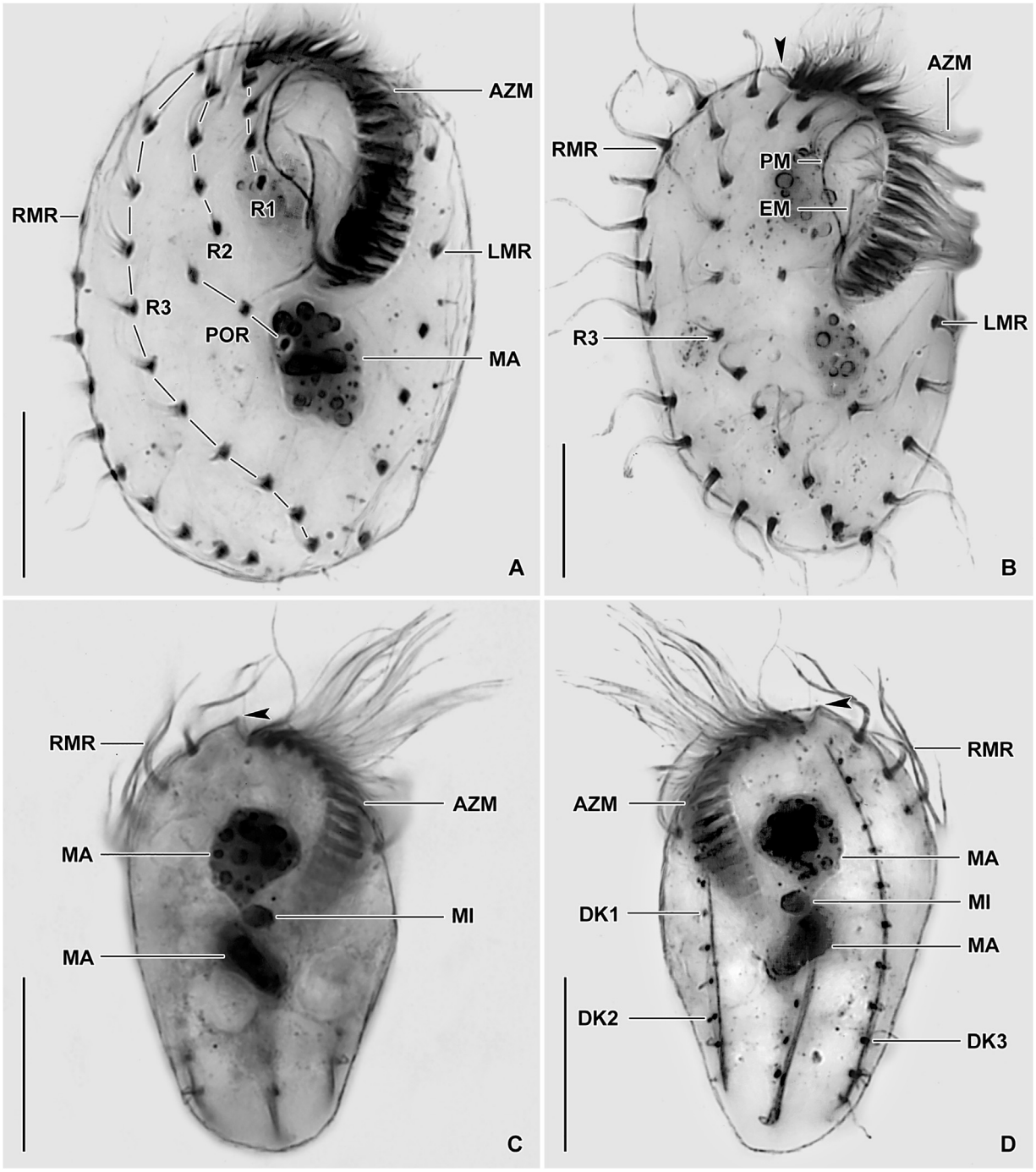

Fig. 9. (**A–D**) *Hemiholosticha germanica* nov. spec. after protargol impregnation. (**A–C**) Ventral overviews, showing the general body organization and the cirral pattern. The nuclear apparatus is situated in the central quarters of the cell and is invariably composed of two macronuclear nodules and one micronucleus in between. There are about 43 cirri arranged in three ventral, one postoral, one right and one left marginal row. (**D**) Dorsal overview, showing the three meridional kineties. Arrowhead in (B–D) marks the anterior body projection. AZM, adoral zone of membranelles; DK1–3, dorsal kineties; EM, endoral membrane; LMR, left marginal cirral row; MA, macronuclear nodules; MI, micronucleus; PM, paroral membrane; POR, postoral cirral row; R1–3, ventral cirral rows; RMR, right marginal cirral row. Scale bars: 20 μm.

sists of three to five cirri, commences subapically and extends to level of or slightly below posterior end of row R1. Ventral cirral row R3 conspicuously longer than R1 and R2; extends from anterior to posterior body end in slightly curved pattern; consists of two unequally long parts separated by a distinct gap: anterior portion invariably composed of two cirri, posterior portion of 8–11 cirri. Postoral cirral row begins slightly posterior to end of row R2, i.e., about at level of proximal end

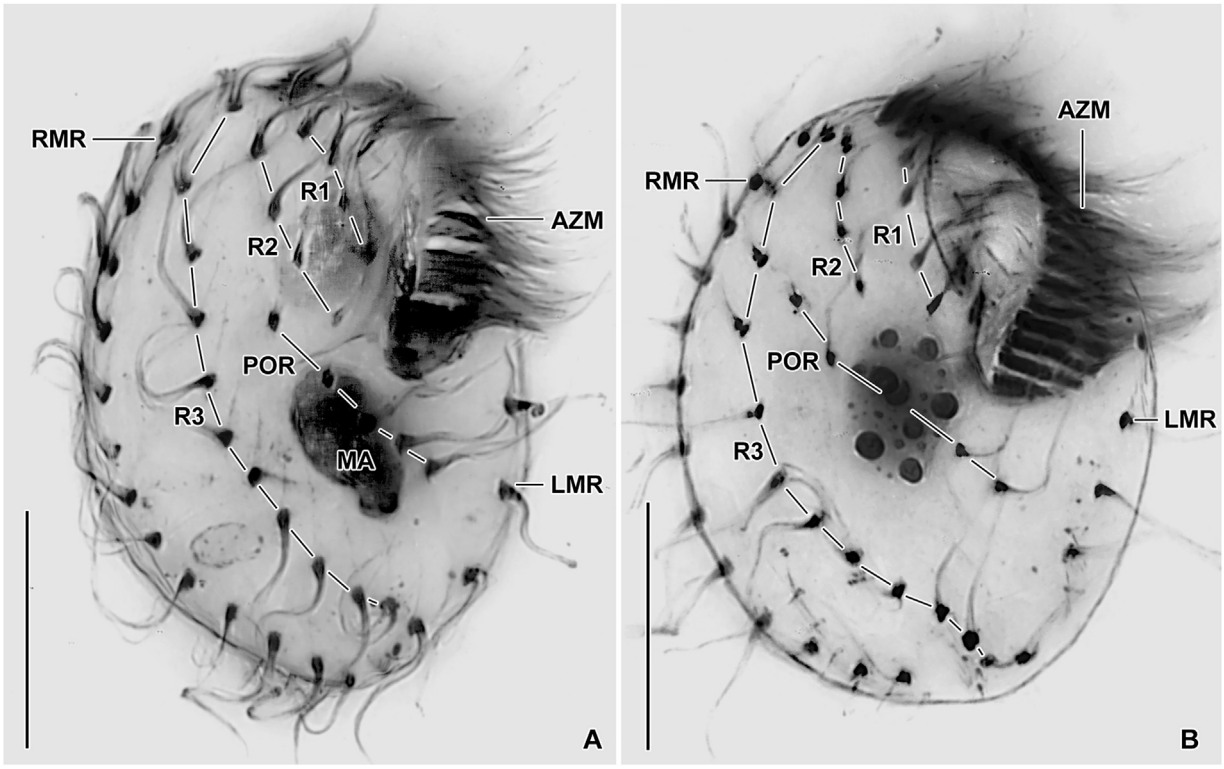

Fig. 10. (**A, B**) *Hemiholosticha germanica* nov. spec. after protargol impregnation. Ventral overviews, showing the general body organization and the cirral pattern. AZM, adoral zone of membranelles; LMR, left marginal cirral row; MA, macronuclear nodule; POR, postoral cirral row; R1–3, ventral cirral rows; RMR, right marginal cirral row. Scale bars: 20 μm.

of adoral zone, extends to end of second third of body; 5–21 μm long after protargol impregnation; composed of two to six, usually five cirri. Right marginal cirral row begins near anterior body end, extends along body margin following its curvature to terminate near rear body end; consists of 9–15 cirri. Left marginal cirral row commences slightly above level of mid-portion of adoral zone and terminates at level of right marginal cirral row; composed of five to eight cirri (Figs. 7B, J, 9A, B, 10A, B; Table 1).

Dorsal bristles fine, increase in length from 3 μm to 4 μm anteriorly to 5–8 μm posteriorly; total number of bristles ranging from 28 to 36 (CV = 7.4%); arranged in three meridional rows; posteriormost bristles of dorsal kinety 2 and 3 protrude beyond rear body end (Fig. 7K, arrows). Dorsal kinety 1 begins in first third of body length, shortened posteriorly, composed of 6–9 bristles. Dorsal kinety 2 commences slightly above dorsal kinety 1, terminates at rear body end, consists of 9–13 bristles. Dorsal kinety 3 starts subapically and extends to posterior body end, consists of 10–16 bristles. Caudal cirri absent (Figs. 7C, K, 9D; Table 1).

Adoral zone extends 51% of body length on average; commences anteriorly near midline of body and forms a question mark-like pattern in ventral view; composed of an average of 18 membranelles. Individual membranelles composed of four rows of basal bodies and of similar structure as in *H. solitaria*; length of membranellar cilia abruptly increases to 17–20 μm in distal half of zone, causing conspicuous frontal membranelles; largest bases of membranelles about 6 μm wide after protargol impregnation (Figs. 7B, H, J, 8A, B, 9A, B, 10A, B; Table 1). Scutum crescentic, inconspicuous, partially covering frontal membranelles. Buccal cavity almost as long as ventral portion of adoral zone; about 4–9 μm wide in protargol preparations. Paroral membrane begins about 5 μm posterior to anterior body end; extends crook-like in cyrtohymenid pattern; about 15 μm long in protargol preparations; composed of narrowly spaced dikinetids. Endoral membrane begins above mid of buccal cavity, i.e., about 12 μm posterior to anterior body end; optically intersects paroral membrane in its proximal portion; about 10 μm long in protargol preparations; composed of densely spaced basal bodies (Figs. 7B, J, 9A, B; Table 1).

Phylogenetic analyses

Maximum likelihood and Bayesian analyses of the 18S rRNA gene of 102 hypotrich and three oligotrich ciliates resulted in highly similar tree topologies, i.e., only five nodes recognised in the Bayesian 50%-majority rule consensus tree were not recovered in the best IQ-tree (Fig. 11). *Psilotricha*, the type genus of the Psilotrichidae, did not cluster with *Hemiholosticha*, *Psilotrichides*, and *Urospinula*. The latter three genera formed a fully statistically supported monophylum, whose common origin was corroborated also by one binary (no. 1408) and two asymmetric

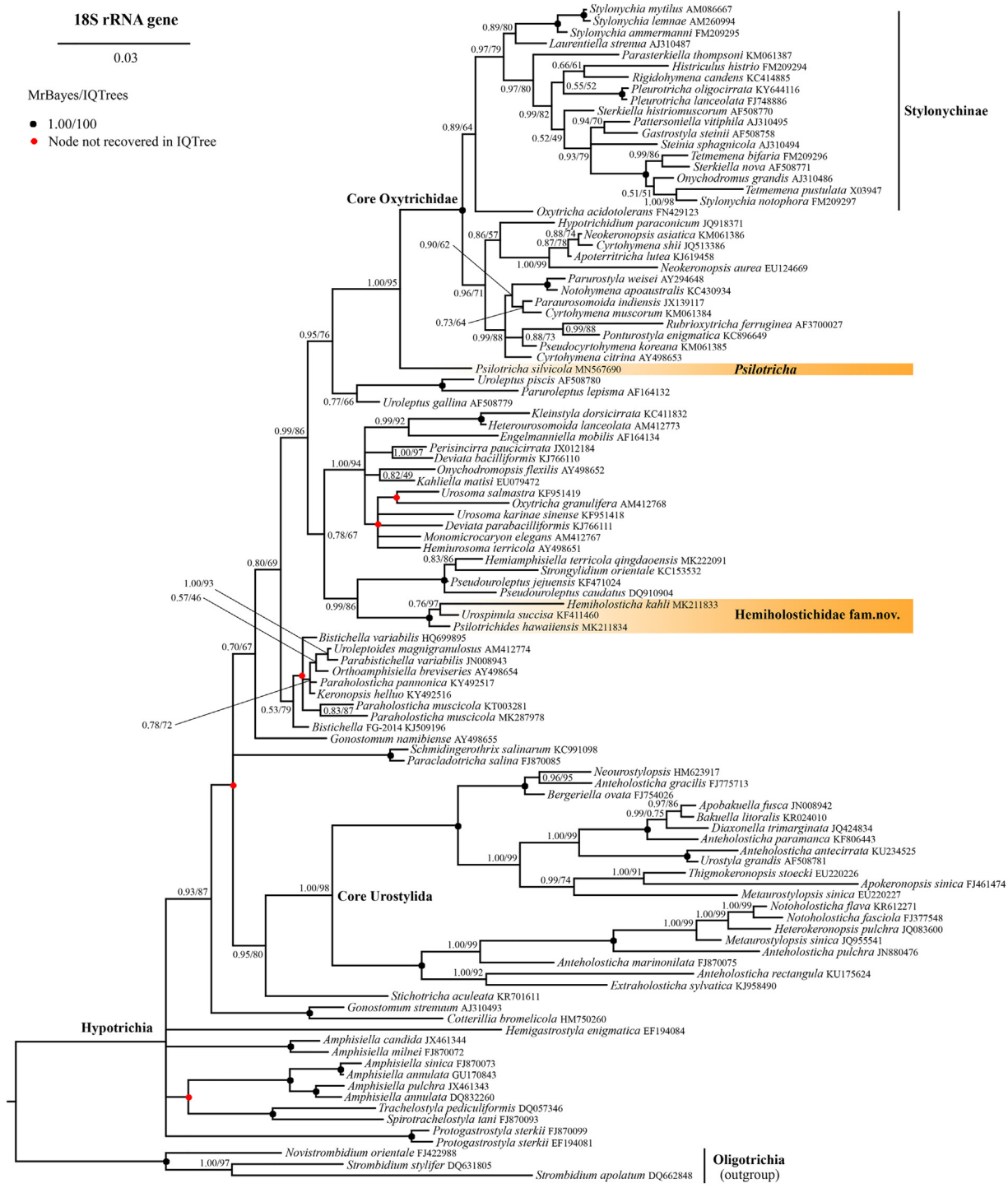

Fig. 11. Nuclear 18S rRNA gene tree, showing the phylogenetic positions of *Hemiholosticha*, *Psilotricha*, *Psilotrichides*, and *Urospinula* within the subclass Hypotrichia. Posterior probabilities for Bayesian inference conducted in MrBayes and bootstrap values for maximum likelihood conducted in IQTrees are mapped onto the 50%-majority rule Bayesian consensus tree. The scale bar denotes three substitutions per one hundred nucleotide positions.

(nos. 836 and 1363) nucleotide positions (Fig. 12). *Hemiholosticha*, *Psilotrichides*, and *Urospinula* grouped together with a clade uniting *Hemiamphisiella terricola qingdaoensis* MK222091, *Strongylidium orientale* KC153532, and two *Pseudouroleptus* species. This morphologically heterogenous cluster obtained moderate to strong statistical support (0.99 MrBayes, 86% IQTrees). On the other hand, *Psilotricha* was depicted in a sister position to the core Oxytrichidae. This grouping received full to strong statistical support (1.00 MrBayes, 95% IQTrees) (Fig. 11).

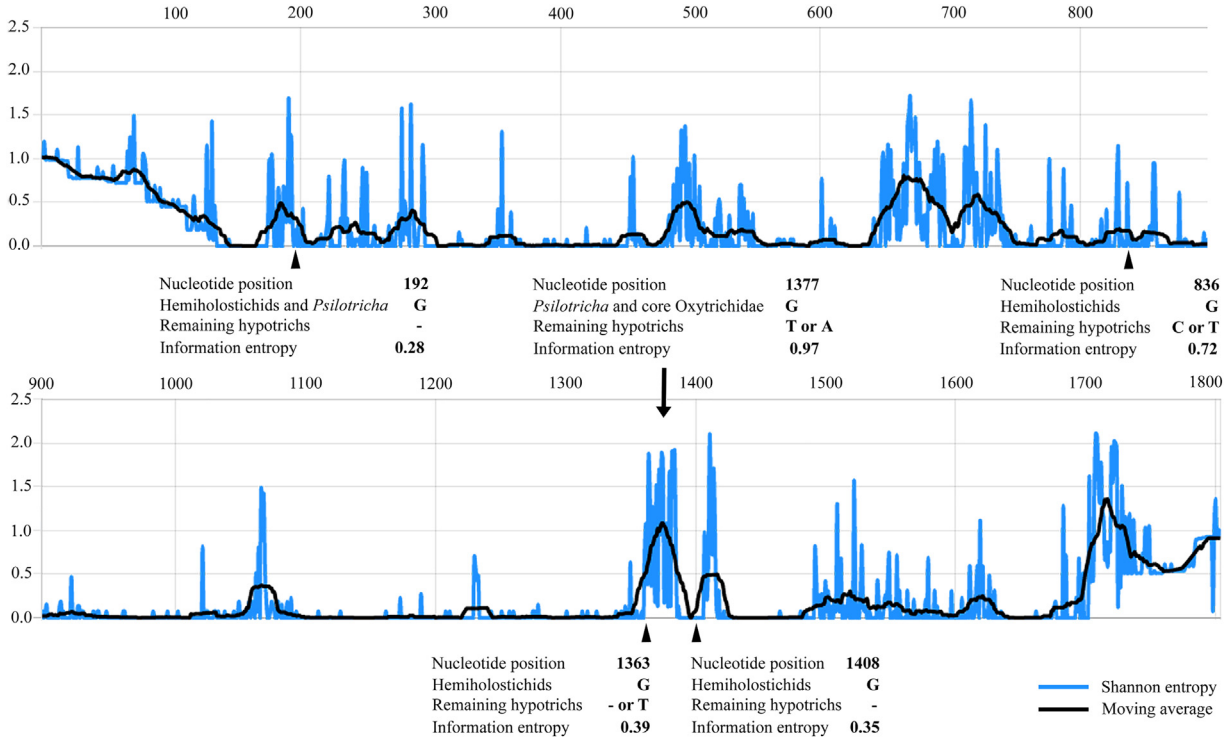

Fig. 12. Entropy plot, showing the position and the character of split-supporting primary nucleotide homologies of hemiholostichids (*Hemiholosticha*, *Psilotrichides*, and *Urospinula*), *Psilotricha*, and the remaining hypotrichs in the 18S rRNA gene alignment. The x-axis represents the nucleotide position in the alignment and the y-axis the Shannon entropy value. High entropy values (peaks) indicate variable alignment regions, while low values indicate conserved regions. A range of five positions was used for calculation of the moving average.

The best IQ-tree in which *Psilotricha* was separated from *Hemiholosticha*, *Psilotrichides* and *Urospinula* had a log likelihood of –13 965.22, while that of the constraint tree in which all four genera were forced to group together was –13 988.15. As the comparison of the log likelihood difference (Δ = 22.93) was not statistically significant (weighted Kishino-Hasegawa test, p = 0.114), the monophyly of the Psilotrichidae sensu Heber et al. (2014) cannot be unambiguously excluded. However, there is a somewhat stronger phylogenetic signal for the unconstraint topology in the 18S rRNA gene alignment. Namely, the grouping of *Psilotricha* with the core Oxytrichidae is corroborated by an asymmetric nucleotide position no. 1377 of the 18S rRNA gene alignment, which involves guanine in the query group and thymine or adenine in the reference group (i.e., all remaining hypotrichs). This position is situated in a variable alignment region, as indicated by the Shannon entropy of 0.97 (moving average 1.03) (Fig. 12). On the other hand, the grouping of *Psilotricha* with *Hemiholosticha*, *Psilotrichides*, and *Urospinula* is corroborated by the nucleotide position no. 192 of the 18S rRNA gene alignment. There is guanine in the query group, while all remaining hypotrichs have there a gap (deletion). Although this region seems to be rather conserved (entropy only 0.28, moving average 0.35) (Fig. 12), multiple taxa exhibit deletions at positions 191 and 193. This is indicative of uncertainties in the alignment and the discriminatory power of this position should be therefore taken with caution. Moreover, 267 noisy nucleotide positions were detected in the case of the first grouping (non-monophyly of psilotrichids), while as many as 438 noisy positions were counted for the second grouping (monophyly of psilotrichids). To summarize, the higher log likelihood value, the character of the primary nucleotide homologies, and the distinctly lower number of noisy nucleotide positions favour separation of *Psilotricha* from *Hemiholosticha*, *Psilotrichides*, and *Urospinula*.

Discussion

The new species *Hemiholosticha solitaria*

Hemiholosticha solitaria nov. spec. is similar to congeners in body shape, the nuclear apparatus, the localization of the contractile vacuole, the organization of the oral apparatus, and in the dorsal ciliary pattern. However, it is outstanding in having four (vs. three) ventral cirral rows. The additional row is labelled as R2 in our diagrams (Fig. 1G) and originates from cirral streak III by migration of its two anteriormost cirri leftwards and anteriorly (Fig. 6A, C, E, arrows). In addition to the higher number of ventral cirral rows, *H. solitaria* can be further separated from *H. germanica* by the number of cirri in ventral rows R1 and R2 (invariably 2 vs. 3–6 cirri in each row). Moreover, *H. solitaria* is distinguished from *H.*

kahli, *H. pantanalensis*, and *H. viridis* by the much higher number of postoral cirri (3–8 vs. typically 2). In addition, *H. viridis* differs from *H. solitaria* by having a distinctly lower number of adoral membranelles (13–14 vs. 19–22) and cirri (19–24 vs. 38–50).

In contrast to all other congeners, *H. solitaria* lacks the intracellular green algae. These have been up to now reported from all other *Hemiholosticha* species including the newly discovered *H. germanica* (Kreutz 2008; Luo et al. 2019; Vďačný and Foissner 2019; present study). The value of the presence/absence of intracellular green algae in the alpha-taxonomy of psilotrichids has not been so far addressed by the means of molecular phylogenetic methods. Nevertheless, our present observations suggest that it might be a good species discriminator, since *H. solitaria* and *H. pantanalensis* co-occurred and only the latter species was associated with intracellular green algae (Vďačný and Foissner 2019). This qualitative difference is supported by morphological (see above) and ontogenetical (see below) data as well. On the other hand, the type population of *Psilotrichides hawaiiensis* contained two colourless, eyespot-bearing, chlamydonomad flagellates *Hyalogonium* and *Polytoma* (Heber et al. 2014), while the Guam population of *P. hawaiiensis* exhibited green, eyespot-bearing algae indistinguishable from those of *H. kahli* from the same site (Luo et al. 2019). Therefore, Luo et al. (2019) speculated that the green algae might have been ingested and represent only selective prey of the Guam population of *P. hawaiiensis*. However, the Guam population is very likely not conspecific with *P. hawaiiensis*, as also indicated by its smaller body size (36–54 × 24–35 μm vs. 50–66 × 34–44 μm after protargol preparation) and the lower number of cirri (17–21 vs. 18–26). Whether the different body size and number of cirri along with the presence/absence of intracellular green algae are population-dependent features, as argued by Luo et al. (2019), or characters documenting that both populations belong to different species, needs to be analysed with molecular methods. Interestingly, molecular data correlate well with the presence/absence of intracellular green algae in other groups of ciliates. For instance, the 18S rRNA gene phylogenies corroborate the separation of the green *Coleps hirtus viridis* Ehrenberg, 1831 from the colourless *C. hirtus hirtus* (Müller, 1876) Nitzsch, 1827 (Yi et al. 2010). Although both taxa are morphologically highly similar (Foissner et al. 1999), molecular analyses suggest that they are not conspecific and *C. hirtus viridis* is more closely related to *C. spetai* Foissner, 1984, which also possesses intracellular green algae, than to the colourless *C. hirtus hirtus* (Yi et al. 2010). Furthermore, molecular data consistently support distinctness of *Spirostomum semivirescens* Perty, 1852 associated with the green alga *Chlorella* sp. (Shazib et al. 2019), *Tetrahymena utriculariae* Pitsch et al., 2017 associated with the green alga *Micractinium* sp. (Pitsch et al. 2017), and of *Paramecium* (*Viridoparamecium*) *chlorelligerum* Kahl, 1935 associated with the green alga *Meyerella* sp. (Kreutz et al. 2012) from their relatives that do not carry intracellular algae. Nevertheless, eco-physiological experiments and molecular phylogenetic analyses are needed to more adequately address the importance of intracellular green/colourless chlamydomonads in the hypotrich alpha-taxonomy.

The new species *Hemiholosticha germanica*

Hemiholosticha germanica nov. spec. highly resembles its congeners in the general body organization. However, it is outstanding in having a much higher number of cirri in ventral rows R1 and R2 (3–6 vs. typically only 2 cirri in each row). Furthermore, *H. germanica* is distinguished from *H. solitaria* by the number of ventral cirral rows (3 vs. 4) and by the presence (vs. absence) of intracellular green algae, and from *H. kahli*, *H. pantanalensis*, and *H. viridis* by the higher number of postoral cirri (2–6, on average 5 vs. typically only 2). In addition, *H. germanica* differs from *H. viridis* by having a distinctly higher number of adoral membranelles (17–20 vs. 13–14) and cirri (37–47 vs. 19–24).

The type population of *H. germanica* was first studied in vivo by Kreutz (2008). He assigned it to *Psilotricha viridis* sensu Kahl (1932) and Penard (1922). Luo et al. (2019) considered their Guam *Hemiholosticha* population to be conspecific with that of Kahl (1932) and Kreutz (2008), and endowed it with a new name, *Hemiholosticha kahli*. However, neither the population studied by Kreutz (2008) nor that investigated by Luo et al. (2019) seems to be conspecific with *P. viridis* sensu Kahl (1932) or the type population of *P. viridis* (= *Balladina viridis*) described by Penard (1922). We studied Kreutz's population also using the protargol impregnation method and have recognised that it represents a new species, *H. germanica*. It differs from *P. viridis* sensu Kahl (1932) by the much larger body (75–95 μm vs. 45–50 μm), the number and localization of micronuclei (a single micronucleus between two macronuclear nodules vs. two micronuclei attached to the lateral side of macronuclear nodules), and the total number of cirri (35 vs. 37–47); from *P. viridis* described by Penard (1922) by the localization of the contractile vacuole (in mid-body vs. at left body margin) and the presence (vs. absence) of transverse cirri; and from *H. kahli* described by Luo et al. (2019) by the much larger body (75–95 μm vs. 50–75 μm) and the higher number of cirri in ventral row R1 (4–6 vs. 2) and R2 (3–5 vs. 3) as well as in the postoral row (2–6 vs. 1–2). The conspecificity of *H. kahli* and *Psilotricha viridis* sensu Kahl (1932) is also to be excluded, because both species clearly differ in the nuclear (a single micronucleus between macronuclear nodules vs. two macronuclear nodules each with a micronucleus) and cirral patterns (three ventral cirral rows, postoral cirral row extends slightly behind the buccal vertex vs. four ventral cirral rows, postoral cirral row extends far behind the buccal vertex).

Comparative ontogenesis

The morphogenetic processes of psilotrichids have been studied in three genera (*Hemiholosticha*, *Psilotrichides*, and

Urospinula), and thoroughly discussed and placed into a phylogenetic context by Foissner (1983), Heber et al. (2014), and Vďačný and Foissner (2019). Their ontogenetic mode is a mixture of some unique features and features found in various groups of hypotrichs (amphisiellids, kahliellids, oxytrichids, and schmidingerothrichids) as well as in other spirotrich subclasses (euplotids and oligotrichs). The ontogenesis of *Hemiholosticha*, *Psilotrichides*, and *Urospinula* can be characterised as follows: (i) the oral primordium develops in a deep pouch as in euplotids and oligotrichs (for a review, see Foissner 1996), (ii) the oral primordium generates one or two cirral streaks in addition to adoral membranelles and undulating membranes (Heber et al. 2014; Vďačný and Foissner 2019), (iii) the undulating membrane anlage does not produce the left frontal cirrus as in euplotids and some schmidingerothrichids (Foissner 2012; Jiang et al. 2010; Lu et al. 2018), (iv) the postoral cirral row originates as a migrating kinetofragment derived from cirral streak III or IV (Foissner 1983; Heber et al. 2014; Vďačný and Foissner 2019; present study), resembling the situation in any hypotrich with at least one postoral cirrus, which typically originates from anlage IV and migrates to the postoral position (e.g., Berger 1999), (v) cirri are not formed from long primary streaks, and (vi) frontal, frontoterminal, buccal, pretransverse, transverse and caudal cirri are not formed (Foissner 1983; Heber et al. 2014; Vďačný and Foissner 2019).

The ontogenesis of individual psilotrichid genera has also a mosaic-like character (Foissner 1983; Heber et al. 2014; Vďačný and Foissner 2019; present study). Specifically, the parental undulating membranes are reorganised and the new postoral cirral row is derived from streak III in *Hemiholosticha* and *Psilotrichides*, while the undulating membranes are not reorganised and the new postoral cirral row is derived from streak IV in *Urospinula*. This indicates that streak III in *Hemiholosticha* and *Psilotrichides* on one hand, and streak IV in *Urospinula* on the other one might not be homologous. The parental postoral cirral row is ontogenetically active and the oral primordium splits two cirral streaks at its right anterior margin in *Hemiholosticha* and *Urospinula*, while the postoral cirral row is inactive and the oral primordium generates only one cirral streak in *Psilotrichides*. Finally, *Hemiholosticha* is unique among the psilotrichids in the composite origin of the longitudinal ventral cirral row R3. This is derived from two anlagen: the anterior portion of ventral cirral row R3 comes from streak III in *H. solitaria* and from streak IV in *H. pantanalensis*, whereas the posterior portion is derived from streak IV in *H. solitaria* and from streak V in *H. pantanalensis* (Vďačný and Foissner 2019; present study). Interestingly, a composite row is formed from similar anlagen in most amphisiellids (Berger 2008) and some kahliellids (Vďačný et al. 2010) (for discussion about numbering and homology of anlagen, see Vďačný and Foissner 2019). Nevertheless, according to the 18S rRNA gene phylogenies, the composite cirral rows evolved very likely convergently in *Hemiholosticha*, amphisiellids, and kahliellids (Heber et al. 2014; Luo et al. 2019).

Although the main morphogenetic processes of *H. solitaria* and *H. pantanalensis* are rather similar and follow the psilotrichid mode, both species differ in the number of cirral streaks (4 vs. 5) and the migration routes of some cirri (Vďačný and Foissner 2019; present study). Our comparative analyses suggest that cirral streaks I and II of both species are homologous, since they are derived from the oral primordium and each streak gives rise to the new ventral cirral row. Cirral streaks III and IV of *H. solitaria* and streaks IV and V of *H. pantanalensis* are also homologous, because they are formed within the parental ventral cirral row R3 and give rise to the new composite cirral row R3 in both species. Consequently, cirral streak III of *H. pantanalensis* can be considered as supernumerary with respect to *H. solitaria*. Streak III of *H. pantanalensis* is generated within the parental cirral row R3 in the proter, while it is derived from the anterior postoral cirrus in the opisthe (Vďačný and Foissner 2019). This cirrus is, however, ontogenetically inactive in *H. solitaria*. A further difference includes the migration routes of cirri derived from the very likely homologous streak III of *H. solitaria* and streak IV of *H. panatanalensis*. More specifically, in *H. solitaria*, streak III first splits two anteriormost cirri that migrate leftwards and anteriorly to form the ventral row R2 (Fig. 6A, C, E, arrows), then it splits four or five further cirri that migrate rightwards and anteriorly to become the anterior part of ventral row R3 (Fig. 6A, C, E, arrowheads), and the remaining cirri migrate leftwards and posteriorly to become the postoral row. In *H. pantanalensis*, streak IV forms only three cirri that migrate rightwards and anteriorly to become the anterior portion of the new ventral row R3. The new postoral cirral row is derived from the supernumerary streak III in *H. pantanalensis* (Vďačný and Foissner 2019). This indicates that even different numbers of cirral streaks and migration routes of cirri can result in a comparatively similar interphase cirral pattern. Therefore, ontogenetic data maybe be crucial to correctly delimit cirral rows in *Hemiholosticha* and, possibly, also to distinguish closely related *Hemiholosticha* species with a similar interphase cirral pattern.

Establishment of the new family Hemiholostichidae

Heber et al. (2014) included *Hemiholosticha*, *Psilotricha*, *Psilotrichides*, and *Urospinula* into the family Psilotrichidae. Evolutionary relationships and systematics of this family are, however, still poorly understood, because detailed morphological and molecular data on *Psilotricha acuminata* Stein, 1859, the type species of *Psilotricha* (by monotypy), are not available. Recently, non-monophyly of the Psilotrichidae was suggested by Luu et al. (2020), as *Psilotricha* did not cluster with *Hemiholosticha*, *Psilotrichides*, and *Urospinula* in their analyses. Although the phylogenetic inferences of Luu

et al. (2020) suffer from multiple methodological problems (e.g., paraphyletic and incorrectly selected out-group, unbalanced taxon sampling, almost complete lack of nodal support, etc.), they included a species of the genus *Psilotricha*, namely *P. silvatica* Luu et al., 2020, into the phylogenetic analyses for the first time. Unfortunately, the generic classification of *P. silvatica* is questionable, because it exhibits frontal and transverse cirri. According to the original description of the genus *Psilotricha* by Stein (1859), there are no frontal and transverse cirri ("Stirn- und Afterwimpern fehlen"). Nevertheless, in the absence of new data on *Psilotricha acuminata*, the re-description by Esteban et al. (2001) should be considered as authoritative and might be assumed that Stein (1859) overlooked frontal and transverse cirri, as the species is rather small.

Luu et al. (2020) suggested that the genus *Psilotricha* does not belong to the family Psilotrichidae but to the Oxytrichidae Ehrenberg, 1838. Moreover, they stated: " family Psilotrichidae would now consist of the genera *Hemiholosticha*, *Psilotrichides* and *Urospinula*". These proposals, however, violate several articles of the International Code of Zoological Nomenclature (International Commission on Zoological Nomenclature, 1999). More specifically, the name-bearing type of the Psilotrichidae is the nominotypical genus *Psilotricha*, as the family-group names is based upon that of the type genus (Article 29 and 63). Moreover, the Principle of Typification (Article 61.1) states that "Each nominal taxon in the family, genus, or species groups has actually or potentially a name-bearing type. The fixation of the name-bearing types of a nominal taxon provides the objective standard of reference for the application of the name it bears." According to Article 61.1.3, once fixed, name-bearing types are stable and provide objective continuity in the application of names. If the argumentation of Luu et al. (2020) is followed in the light of the International Code of Zoological Nomenclature, the family-group name Psilotrichidae would become a junior, subjective synonym of the Oxytrichidae, and a new family-group name needs to be established for *Hemiholosticha*, *Psilotrichides*, and *Urospinula*. In the present study, we, therefore, propose a new family-group name, Hemiholostichidae, to unite these three peculiar hypotrich genera.

The separation of *Hemiholosticha*, *Psilotrichides*, and *Urospinula* from *Psilotricha* is justified both in the morphological and the molecular point of view. Thus, hemiholostichids differ from *Psilotricha*, as characterised by Esteban et al. (2001) and Luu et al. (2020), by the absence (vs. presence) of frontal, transverse, and caudal cirri as well as by having a postoral row composed of multiple cirri (vs. one postoral ventral cirrus). Molecular data support the establishment of the Hemiholostichidae in that *Hemiholosticha*, *Psilotrichides*, and *Urospinula* form a fully statistically supported cluster, whose monophyly is also sustained by one binary (no. 1408) and two asymmetric (nos. 836 and 1363) nucleotide positions (Fig. 12). And, finally, the separation of hemiholostichids from *Psilotricha* is corroborated by the higher log likelihood value (log likelihood difference Δ = 22.93), the character of the clade-supporting primary nucleotide homologies, and the distinctly lower number of noisy nucleotide positions (267 vs. 438).

Taxonomic summary

Family Hemiholostichidae nov. fam.

ZooBank registration number

urn:lsid:zoobank.org:act:1D1422 F6−0FFA-4BF0-B444−9B87 F0ACE541.

Diagnosis

Medium-sized, ellipsoid hypotrichs with posterior body end rounded, acute, or with one or two spines. Two macronuclear nodules, usually one micronucleus in between. Contractile vacuole at left body margin or near body centre slightly posterior of buccal vertex. Cortex rigid, in some species with distinct ridges. Cirri long and sparse, arranged in several ventral rows, one postoral row, one right and one left marginal row. Three to five dorsal kineties; dorsomarginal kineties and caudal cirri absent. Oral primordium invaginates into a pouch and generates one or two cirral streaks in addition to adoral membranelles and undulating membranes; undulating membrane anlage does not produce left frontal cirrus; postoral cirral row originates as a migrating kinetofragment derived from cirral streak III or IV; cirri are not formed from long primary streaks; frontal, frontoterminal, buccal, pretransverse, transverse and caudal cirri are not formed.

Type genus

Hemiholosticha Gelei, 1954.

Genera assignable

Hemiholosticha Gelei, 1954; *Psilotrichides* Heber et al., 2018; and *Urospinula* Corliss, 1960.

Remarks

Pachycirrus costatus Olmo and Esteban, 1999 (*Psilotricha acuminata* according to Esteban et al. 2001) and *Balladina viridis* Penard, 1922, the type species of *Pigostyla* Tagliani, 1922, are excluded from the Hemiholostichichae, because they possess transverse cirri. For further details, nomenclatural and taxonomic history, see Berger (1999), Aescht (2001), and Heber et al. (2014).

Author contributions

W.F. made the in vivo observations, micrographs, and all preparations. P.V. analysed the protargol-impregnated slides

and SEM micrographs, prepared the manuscript, and all figure plates.

CRediT authorship contribution statement

Peter Vďačný: Conceptualization, Formal analysis, Funding acquisition, Project administration, Investigation, Visualization, Writing – original draft, review & editing. **Wilhelm Foissner:** Conceptualization, Investigation, Methodology, Supervision.

Acknowledgements

This study had been initiated about 15 years ago. The passing of Wilhelm Foissner impeded our plans, but the junior author wishes to accomplish the manuscript in Willi's honour. We are grateful to Dr. Michael Gruber and Robert Schörghofer for technical assistance, and to Maria Pichler, Birgit Weissenbacher, and Martin Kreutz for providing the terrestrial and aquatic samples. This work was supported by the Slovak Research and Development Agency under contracts No. APVV-15-0147 and APVV-19-0076 as well as by the Grant Agency of the Ministry of Education, Science, Research and Sport of the Slovak Republic and Slovak Academy of Sciences under the Grant VEGA 1/0041/17. Additional support was provided by the Wilhelm and Ilse Foissner Stiftung.

References

Aescht, E., 2001. Catalogue of the generic names of ciliates (Protozoa, Ciliophora). Denisia 1, 1–350.

Berger, H., 1999. Monograph of the Oxytrichidae (Ciliophora, Hypotrichia). Monogr. Biol. 78, 1–1080.

Berger, H., 2006. Monograph of the Urostyloidea (Ciliophora, Hypotricha). Monogr. Biol. 85, 1–1304.

Berger, H., 2008. Monograph of the Amphisiellidae and Trachelostylidae (Ciliophora, Hypotricha). Monogr. Biol. 88, 1–737.

Berger, H., 2011. Monograph of the Gonostomatidae and Kahliellidae (Ciliophora, Hypotricha). Monogr. Biol. 90, 1–741.

Darriba, D., Taboada, G.L., Doallo, R., Posada, D., 2012. jModelTest 2: more models, new heuristics and parallel computing. Nat. Methods 9, 772.

Esteban, G.F., Olmo, J.L., Finlay, B.J., 2001. Redescription of *Psilotricha acuminata* Stein, 1859 and revisions of the genera *Psilotricha* and *Urospinula* (Ciliophora, Hypotrichida). J. Eukaryot. Microbiol. 48, 280–292.

Foissner, W., 1983. Morphologie und Morphogenese von *Psilotricha succisa* (O. F. Müller, 1786) nov. comb. (Ciliophora, Hypotrichida). Protistologica 19, 479–493.

Foissner, W., 1991. Basic light and scanning electron microscopic methods for taxonomic studies of ciliated protozoa. Eur. J. Protistol. 27, 313–330.

Foissner, W., 1996. Ontogenesis in ciliated protozoa, with emphasis on stomatogenesis. In: Hausmann, K., Bradbury, B.C. (Eds.), Ciliates: Cells as Organisms. Fischer Verlag, Stuttgart, Jena, New York, pp. 95–177.

Foissner, W., 2014. An update of 'basic light and scanning electron microscopic methods for taxonomic studies of ciliated protozoa'. Int. J. Syst. Evol. Microbiol. 64, 271–292.

Foissner, W., 2012. *Schmidingerothrix extraordinaria* nov. gen., nov. spec., a secondarily oligomerized hypotrich (Ciliophora, Hypotricha, Schmidingerotrichidae nov. fam.) from hypersaline soils of Africa. Eur. J. Protistol. 48, 237–251.

Foissner, W., 2016. Terrestrial and semiterrestrial ciliates (Protozoa, Ciliophora) from Venezuela and Galápagos. Denisia 35, 1–912.

Foissner, W., Agatha, S., Berger, H., 2002. Soil ciliates (Protozoa, Ciliophora) from Namibia (Southwest Africa), with emphasis on two contrasting environments, the Etosha region and the Namib Desert. Denisia 5, 1–1459.

Foissner, W., Berger, H., Schaumburg, J., 1999. Identification and Ecology of Limnetic Plankton Ciliates. Informationsberichte des Bayer. Landesamtes für Wasserwirtschaft 3/99, pp. 1–793.

Heber, D., Stoeck, T., Foissner, W., 2014. Morphology and ontogenesis of *Psilotrichides hawaiiensis* nov. gen., nov. spec. and molecular phylogeny of the Psilotrichidae (Ciliophora, Hypotrichia). J. Eukaryot. Microbiol. 61, 260–277.

Hoang, D.T., Chernomor, O., von Haeseler, A., Minh, B.Q., Vinh, L.S., 2018. UFBoot2: improving the ultrafast bootstrap approximation. Mol. Biol. Evol. 35, 518–522.

Hu, X., Warren, A., Song, W., 2009. Hypotrichs. In: Song, W., Warren, A., Hu, X. (Eds.), Free-Living Ciliates in the Bohai and Yellow Seas, China. Science Press, Beijing, pp. 353–413.

Hütter, T., Ganser, M.H., Kocher, M., Halkic, M., Agatha, S., Augsten, N., 2020. DeSignate: detecting signature characters in gene sequence alignments for taxon diagnoses. BMC Bioinform. 21, 151.

International Commission on Zoological Nomenclature, 1999. International Code of Zoological Nomenclature, 4th ed. Tipografia La Garangola, Padova.

International Commission on Zoological Nomenclature, 2012. Amendment of Articles 8, 9, 10, 21 and 78 of the International Code of Zoological Nomenclature to expand and refine methods of publication. Bull. Zool. Nomencl. 69, 161–169.

Jiang, J., Shao, C., Xu, H., Al-Rasheid, K.A.S., 2010. Morphogenetic observations on the marine ciliate *Euplotes vannus* during cell division (Protozoa: Ciliophora). J. Mar. Biol. Assoc. U.K. 90, 683–689.

Jung, J.-H., Berger, H., 2019. Monographic treatment of *Paraholosticha muscicola* (Ciliophora, Keronopsidae), including morphological and molecular biological characterization of a brackish water population from Korea. Eur. J. Protistol. 68, 48–67.

Kahl, A., 1932. Urtiere oder Protozoa I: Wimpertiere oder Ciliata (Infusoria) 3. Spirotricha. Tierwelt Dtl. 25, 399–650.

Katoh, K., Rozewicki, J., Yamada, K.D., 2019. MAFFT online service: multiple sequence alignment, interactive sequence choice and visualization. Brief. Bioinform. 20, 1160–1166.

Kreutz, M., 2008. *Psilotricha viridis* - Ein Ciliat mit außergewöhnlichen Zoochlorellen. Mikrokosmos 97, 328–333.

Kreutz, M., Foissner, W., 2006. The *Sphagnum* ponds of Simmelried in Germany: a biodiversity hot-spot for microscopic organisms. Protozool. Monogr. 3, 1–267.

Kreutz, M., Stoeck, T., Foissner, W., 2012. Morphological and molecular characterization of *Paramecium* (*Viridoparame-*

cium nov. subgen.) *chlorelligerum* Kahl 1935 (Ciliophora). J. Eukaryot. Microbiol. 59, 548–563.

Liu, W., Jiang, J., Xu, Y., Pan, X., Qu, Z., Luo, X., El-Serehy, H.A., Warren, A., Ma, H., Pan, H., 2017. Diversity of free-living marine ciliates (Alveolata, Ciliophora): faunal studies in coastal waters of China during the years 2011–2016. Eur. J. Protistol. 61, 424–438.

Lu, X., Huang, J.A., Shao, C., Berger, H., 2018. Morphology, cell-division, and phylogeny of *Schmidingerothrix elongata* spec. nov. (Ciliophora, Hypotricha), and brief guide to hypotrichs with *Gonostomum*-like oral apparatus. Eur. J. Protistol. 62, 24–42.

Luo, X., Huang, J.A., Li, L., Song, W., Bourland, W.A., 2019. Phylogeny of the ciliate family Psilotrichidae (Protista, Ciliophora), a curious and poorly-known taxon, with notes on two algae-bearing psilotrichids from Guam, USA. BMC Evol. Biol. 19, 125.

Luu, H.T.T., Quintela-Alonso, P., Sendra, K., Green, I.D., Esteban, G.F., 2020. Morphology and phylogeny of the ciliate *Psilotricha silvicola* n. sp. (Alveolata, Ciliophora) from woodland soils in the United Kingdom. Protist 171, 125752.

Lynn, D.H., 2008. The Ciliated Protozoa. Characterization, Classification and Guide to the Literature, 3rd ed. Springer, Dordrecht.

Miller, M.A., Pfeiffer, W., Schwartz, T., 2010. Creating the CIPRES science gateway for inference of large phylogenetic trees. In: Proceedings of the Gateway Computing Environments Workshop (GCE), New Orleans, LA, pp. 1–8.

Nguyen, L.T., Schmidt, H.A., von Haeseler, A., Minh, B.Q., 2015. IQ-TREE: a fast and effective stochastic algorithm for estimating maximum-likelihood phylogenies. Mol. Biol. Evol. 32, 268–274.

Penard, E., 1922. Études Sur Les Infusoires d'Eau Douce. Georg & Cie, Genève.

Pitsch, G., Adamec, L., Dirren, S., Nitsche, F., Šimek, K., Sirová, D., Posch, T., 2017. The green *Tetrahymena utriculariae* n. sp. (Ciliophora, Oligohymenophorea) with its endosymbiotic algae (*Micractinium*sp.), living in traps of a carnivorous aquatic plant. J. Eukaryot. Microbiol. 64, 322–335.

Ronquist, F., Teslenko, M., van der Mark, P., Ayres, D.L., Darling, A., Höhna, S., Larget, B., Liu, L., Suchard, M.A., Huelsenbeck, J.P., 2012. MrBayes 3.2: efficient Bayesian phylogenetic inference and model choice across a large model space. Syst. Biol. 61, 539–542.

Shazib, S.U.A., Vďačný, P., Slovák, M., Gentekaki, E., Shin, M.K., 2019. Deciphering phylogenetic relationships and delimiting species boundaries using a Bayesian coalescent approach in protists: a case study of the ciliate genus *Spirostomum* (Ciliophora, Heterotrichea). Sci. Rep. 9, 16360.

Stein, F., 1859. Characteristik neuer Infusorien-Gattungen. Lotos 9, 57–60.

Vďačný, P., Foissner, W., 2012. Monograph of the dileptids (Protista, Ciliophora, Rhynchostomatia). Denisia 31, 1–529.

Vďačný, P., Foissner, W., 2019. Morphology and ontogenesis of *Hemiholosticha pantanalensis* nov. spec. (Ciliophora, Hypotrichia, Psilotrichidae). Acta Protozool. 58, 93–113.

Vďačný, P., Tirjaková, E., Tóthová, T., Pristaš, P., Javorský, P., 2010. Morphological and phylogenetical studies on a new soil hypotrich ciliate: *Kahliella matisi* spec. nov. (Hypotrichia, Kahliellidae). Eur. J. Protistol. 46, 319–333.

Yi, Z., Dunthorn, M., Song, W., Stoeck, T., 2010. Increasing taxon sampling using both unidentified environmental sequences and identified cultures improves phylogenetic inference in the Prorodontida (Ciliophora, Prostomatea). Mol. Phylogenet. Evol. 57, 937–941.